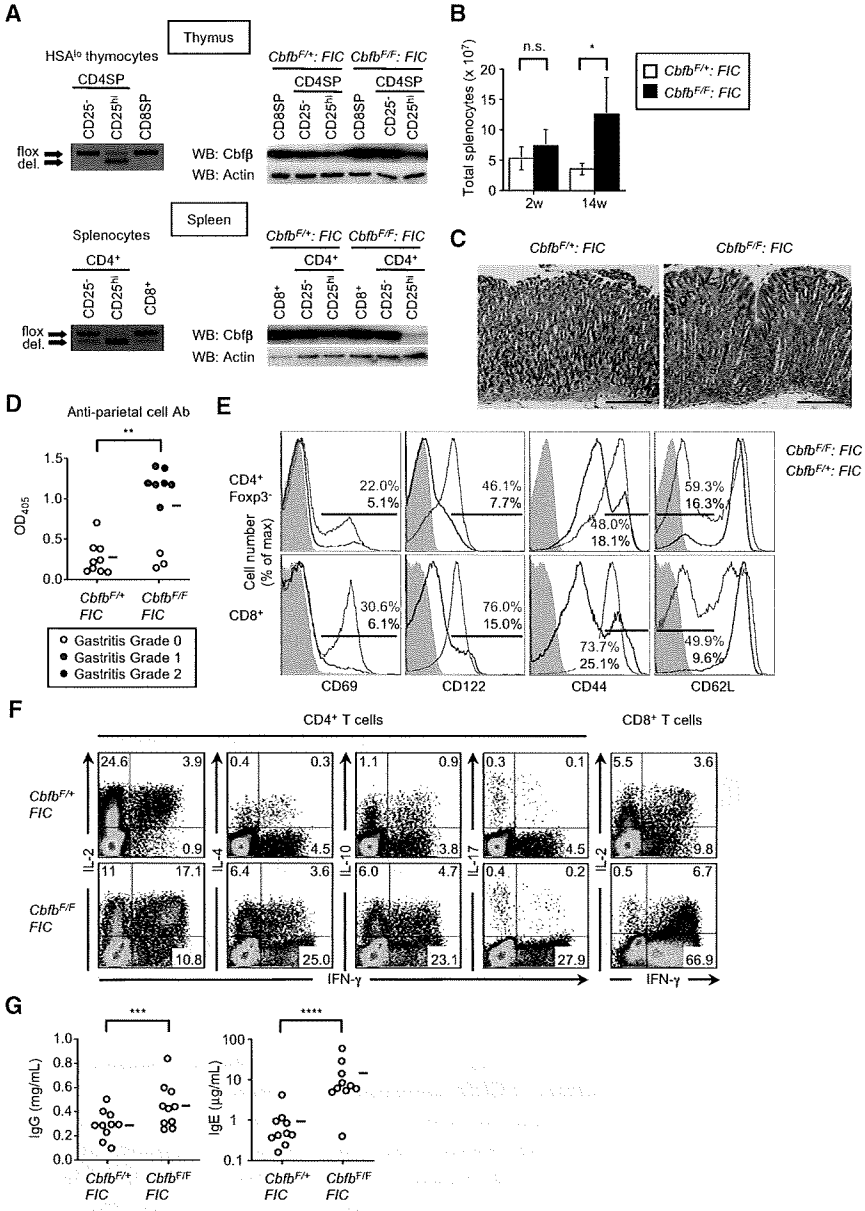

Figure 1. Treg Cell-Specific *Cbfb* Deficiency Induced Autoimmune Disease and Hyperproduction of IgE

(A) Treg cell-specific *Cbfb* deletion in *Cbfb*$^{F/F}$*: FIC* mice. PCR analysis (left) for detecting *Cbfb*^{F} (flox) and *Cbfb*-deleted (del.) alleles of the *Cbfb* gene was performed with genomic DNA from indicated thymocyte (top) and splenocyte (bottom) subpopulations of *Cbfb*$^{F/F}$*: FIC* mice as templates. Immunoblot analysis (right) of Cbfβ protein expression in indicated thymocyte (top) and splenocyte (bottom) subpopulations of *Cbfb*$^{F/F}$*: FIC* and control *Cbfb*$^{F/+}$*: FIC* littermates is shown. Results representative of two experiments are shown.

(B) The absolute numbers of total splenocytes are shown as the mean ± SD value from *Cbfb*$^{F/F}$*: FIC* mice and *Cbfb*$^{F/+}$*: FIC* littermates (n = 4) at 2 and 14 weeks of age. *p = 0.02.

(C) Hematoxylin and eosin staining of sections from stomachs of 7- to 8-week-old *Cbfb*$^{F/F}$*: FIC* and *Cbfb*$^{F/+}$*: FIC* littermates (n = 10). Representative photomicrographs are shown. Scale bars represent 10.0 μm.

(D) Titers of parietal cell autoantibodies in the sera of 8-week-old *Cbfb*$^{F/F}$*: FIC* and *Cbfβ*$^{F/+}$*: FIC* littermates (n = 10) were assessed by ELISA. Horizontal lines represent averages from each group. **p = 0.01.

(E) Activated surface-marker phenotype of CD4^{+}FoxP3^{-} conventional T cells and CD8^{+} T cells in *Cbfb*$^{F/F}$*: FIC* mice at 16 weeks of age. Data are representative of five experiments.

(F) Production of proinflammatory cytokines by CD4^{+} and CD8^{+} T cells in *Cbfb*$^{F/F}$*: FIC* mice at 14 weeks of age. Data are representative of three experiments.

(G) Titers of IgG and IgE in the sera of 8-week-old *Cbfb*$^{F/F}$*: FIC* and *Cbfb*$^{F/+}$*: FIC* littermates (n = 10) were assessed by ELISA. Horizontal lines represent averages from each group. ***p = 0.04; ****p = 0.001.

Treg cells in *Runx1*$^{F/F}$*: Cd4-Cre* mice were apoptosis resistant (Egawa et al., 2007) (Figures 2G and 2H).

Phenotypically, *Cbfb*-deleted Treg cells expressed CD25 and glucocorticoid-induced tumor necrosis factor receptor family-related protein (GITR) at higher amounts and CTLA-4 at equivalent amounts compared to control Treg cells, whereas they scarcely expressed CD103 in accord with the finding that Runx3 controls CD103 expression (Grueter et al., 2005) (Figure 3A). Neither *Cbfb*-deleted nor control Treg cells proliferated in response to in vitro polyclonal TCR stimulation with anti-CD3 (Figure 3B). Yet, *Cbfb*-deleted Treg cells were less suppressive in vitro (Figure 3C). In addition, they failed to prevent the development of colitis and weight loss in SCID mice when cotransferred with BALB/c CD4^{+}CD25^{-}CD45RB^{hi} T cells, in contrast to effective disease prevention by cotransfer of control Treg cells (Figures 3D–3F). Similarly, *Cbfb*-deleted Treg cells failed to suppress the development of gastritis (data not shown). *Cbfb*-deleted Treg cells survived when transferred to SCID mice (Figure S5A), indicating that the impaired in vivo suppressive activity of *Cbfb*-deleted Treg cells was not due to their shorter survival. In addition, the attenuated CD103 expression in *Cbfb*-deleted Treg cells (Figure S5B) would not be responsible for the impaired Treg cell function because others reported that Treg cell-mediated control of colitis did not require CD103 expression by Treg cells (Annacker et al., 2005).

Collectively, these findings indicate that failure in Treg cell-mediated self-tolerance in *Cbfb*$^{F/F}$*: FIC* mice is not due to numerical deficiency, reduced proliferation, or enhanced apoptosis of FoxP3^{+} Treg cells, but due to their impaired suppressive activity.

Cbfb-Deleted Treg Cells Show Hyperproduction of IL-4

Treg cells hardly produce cytokines such as IL-2, IFN-γ, and IL-4 (Sakaguchi et al., 2006). Flow cytometric analysis revealed that a larger proportion of FoxP3^{+} Treg cells from *Cbfb*$^{F/F}$*: FIC* mice produced IL-4 and IL-10 compared to Treg cells from control

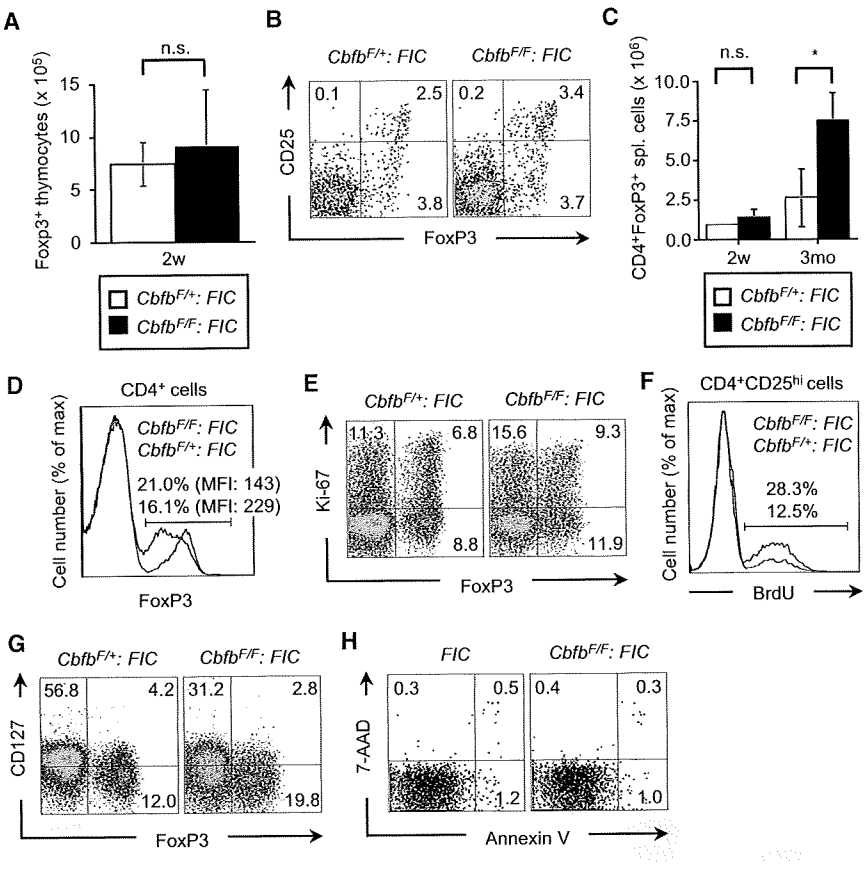

Figure 2. Generation and Homeostasis of Treg Cells in *Cbfb*$^{F/F}$: *FIC* Mice

(A) The absolute numbers of FoxP3$^+$ thymocytes from 2-week-old *Cbfb*$^{F/F}$: *FIC* and *Cbfb*$^{F/+}$: *FIC* littermates (n = 3) are shown as the mean ± SD value.

(B) Expression of CD25 and FoxP3 by CD4SP HSA^{lo} thymocytes from 3-week-old *Cbfb*$^{F/F}$: *FIC* and *Cbfb*$^{F/+}$: *FIC* littermates. Results representative of three experiments are shown.

(C) The absolute numbers of CD4$^+$FoxP3$^+$ splenocytes from *Cbfb*$^{F/F}$: *FIC* and *Cbfb*$^{F/+}$: *FIC* littermates (n = 3) at 2 weeks and 3 months of age are shown as the mean ± SD value. *p = 0.05.

(D) Expression of FoxP3 by CD4$^+$ splenocytes from 7-week-old *Cbfb*$^{F/F}$: *FIC* and *Cbfb*$^{F/+}$: *FIC* littermates. Results representative of five experiments are shown.

(E) Expression of Ki-67 and FoxP3 by CD4$^+$ T cells from 7-week-old *Cbfb*$^{F/F}$: *FIC* and *Cbfb*$^{F/+}$: *FIC* littermates. Data are representative of three experiments.

(F) 9-week-old *Cbfb*$^{F/F}$: *FIC* and *Cbfb*$^{F/+}$: *FIC* littermates were injected with BrdU for 3 days, and incorporation of BrdU into CD4$^+$CD25^{hi} splenocytes was assessed by flow cytometry. Results representative of four experiments are shown.

(G) Expression of CD127 and FoxP3 by CD4$^+$ T cells from 7-week-old *Cbfb*$^{F/F}$: *FIC* and *Cbfb*$^{F/+}$: *FIC* littermates. Results representative of four experiments are shown.

(H) 7-AAD and AnnexinV staining of CD4$^+$CD25^{hi} cells from 8-week-old *Cbfb*$^{F/F}$: *FIC* and littermate control mice. Results representative of two experiments are shown.

mice, whereas there were no substantial differences in the percentage of IL-2- or IFN-γ-producing cells among FoxP3$^+$ Treg cells (Figure 3G). Few IL-17-expressing FoxP3$^+$ Treg cells were present in both groups of mice (Figure 3G). The amount of mRNA for each cytokine in CD4$^+$CD25^{hi} cells in *Cbfb*$^{F/F}$: *FIC* and control mice correlated with the protein expression. However, mRNA for IL-17, which was detectable in *Cbfb*$^{F/+}$: *FIC* mice, was substantially lower in *Cbfb*$^{F/F}$: *FIC* mice (Figure 3H).

Next, the expression of transcription factors *Foxp3*, *Tbx21*, *Gata3*, and *Rorgt*, all of which are essential for Th or Treg cell lineage differentiation, were examined in *Cbfb*-deleted Treg cells. *Foxp3* mRNA expression decreased in *Cbfb*-deleted Treg cells, which is consistent with decreased FoxP3 expression at the protein level (Figure S6). In contrast to the hyperproduction of Th2 cell cytokines IL-4 and IL-10, mRNA expression of Th2 cell-specific transcription factor *Gata3* in *Cbfb*-deleted Treg cells was equivalent to that in control Treg cells, whereas *Cbfb*-deleted Treg cells showed higher expression of Th1 cell-specific transcription factor *Tbx21*. Thus, hyperproduction of Th2 cell cytokines by *Cbfb*-deleted Treg cells was not due to overexpression of *Gata3*, although it has been reported that Runx1 represses *Gata3* expression in conventional CD4$^+$ T cells (Komine et al., 2003). The expression of *Rorgt*, which controls the differentiation of IL-17-producing Th17 cells, also decreased in *Cbfb*-deleted Treg cells compared with control Treg cells (Figure S6). Taken together, our findings show that Cbfβ-deficient Treg cells transcribed *Il17a* and *Rorgt* to lesser extents than control Treg cells, whereas *Il4*, *Il10*, and *Tbx21* were more actively transcribed in the former.

Genes Possibly Associated with Impaired Suppressive Function of *Cbfb*-Deleted Treg Cells

To elucidate the molecular mechanisms underlying the dysfunction of *Cbfb*-deleted Treg cells, we examined gene expression profiles of CD4$^+$CD25^{hi} cells from *Cbfb*$^{F/F}$: *FIC* and littermate *Cbfb*$^{F/+}$: *FIC* mice by expression microarray. We first focused on the previously described "Treg cell signature" genes, which are differentially expressed between Treg cells and conventional CD4$^+$ T cells and therefore thought to be closely related to Treg cell-intrinsic properties including suppressive function (Hill et al., 2007). Sixty-nine signature genes including *Socs2* and *Nrp1* were found to be differentially expressed in *Cbfb*-deleted Treg cells (unpaired t test, $p < 0.05$. see Table S1). Yet, there were not significant differences in the expression of many well-known Treg cell-associated genes, such as *Ctla4*, *Tnfrsf18* (*Gitr*), *Gzmb*, *Folr4*, and *Gpr83*, between *Cbfb*-deleted and control Treg cells (Figure 4A). Decreased mRNA expression of *Itgae* (*CD103*) in *Cbfb*-deleted Treg cells was consistent with the aforementioned flow cytometry results (Figure 4A and Figure 3A). Using the false discovery rate (FDR)-controlling procedure (FDR < 0.2), we further attempted to determine other genes that were differentially expressed in *Cbfb*-deleted Treg cells. We found that 22 and 24 genes were significantly up- or

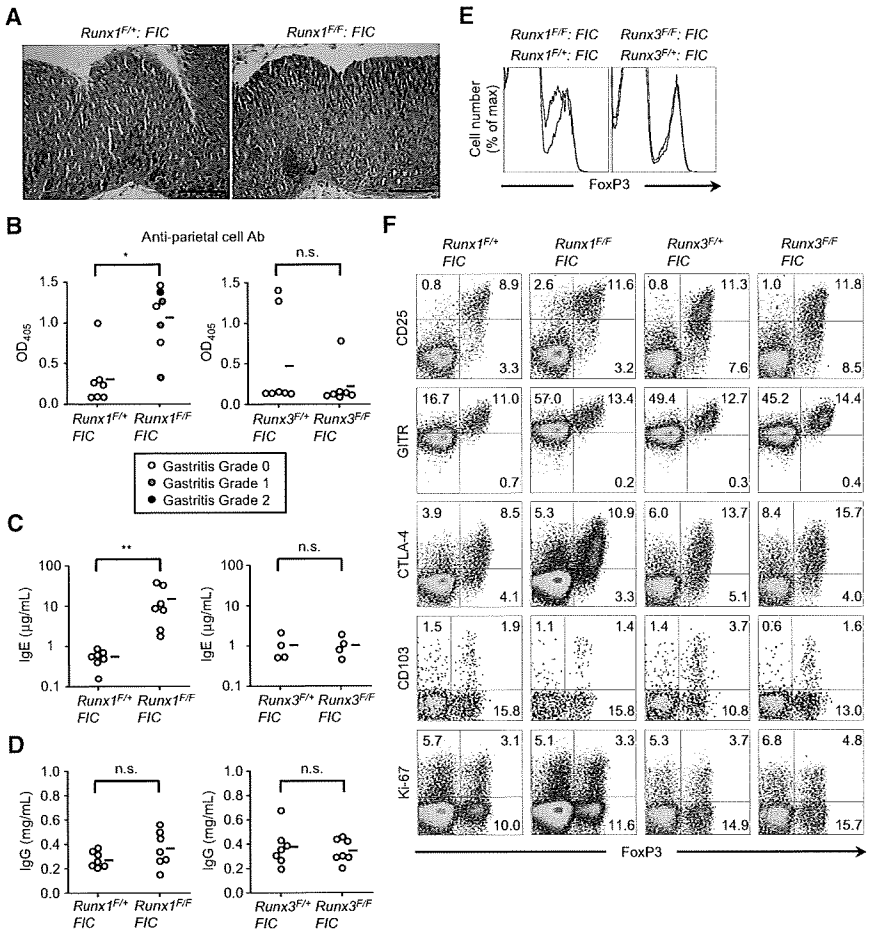

Figure 7. Development of Autoimmune Disease and Hyperproduction of IgE in *Runx1$^{F/F}$: FIC* Mice, but Not in *Runx3$^{F/F}$: FIC* Mice

(A) Hematoxylin and eosin staining of stomach sections of 8- to 9-week-old *Runx1$^{F/F}$: FIC* and *Runx1$^{F/+}$: FIC* littermates (n = 7). Representative photomicrographs are shown. Scale bars represent 10.0 μm.

(B) Titers of parietal cell autoantibodies in the sera of 8- to 9-week-old *Runx1$^{F/F}$: FIC* and *Runx1$^{F/+}$: FIC* littermates (n = 7) (left) and *Runx3$^{F/F}$: FIC* and *Runx3$^{F/+}$: FIC* littermates (n = 7) (right) were assessed by ELISA. Horizontal lines represent averages from each group. *p = 0.01.

(C and D) Titers of IgE (C) and IgG (D) in the sera of 8- to 9-week-old *Runx1$^{F/F}$: FIC* and *Runx1$^{F/+}$: FIC* littermates (n = 7) and *Runx3$^{F/F}$: FIC* and *Runx3$^{F/+}$: FIC* littermates (n = 4) were assessed by ELISA. Horizontal lines represent averages from each group. **p = 0.002.

(E) Flow cytometric analysis of FoxP3 expression by CD4$^+$ T cells from *Runx1$^{F/F}$: FIC* and *Runx1$^{F/+}$: FIC* littermates (left) and from *Runx3$^{F/F}$: FIC* and *Runx3$^{F/+}$: FIC* littermates (right) at 7 weeks of age. Results representative of three experiments are shown.

(F) Expression of FoxP3 and the indicated molecules by *Runx1$^{F/F}$: FIC* and *Runx1$^{F/+}$: FIC* littermates and by *Runx3$^{F/F}$: FIC* and *Runx3$^{F/+}$: FIC* littermates at 7 to 10 weeks of age. Results representative of three experiments are shown.

We have previously shown that Runx1 binds to the promoter of the *Il2* and *Ifng* genes and enhances IL-2 and IFN-γ production in conventional T cells. Conversely, the FoxP3-Runx1 complex, together with other transcription factors such as NFAT, represses the expression of these cytokines and confers in vitro-suppressive activity to Treg cells (Ono et al., 2007). Here, we have provided genetic evidence that Treg cell-specific deficiency of the Runx1-Cbfβ complex indeed impairs in vivo Treg cell function. This indicates that Runx-dependent gene regulation is critically required for in vivo Treg cell function. In addition, Cbfβ-deficient Treg cells transcribed *Il17a* and *Rorgt* to lesser extents than control Treg cells, whereas *Il4*, *Il10*, and *Tbx21* increased in the former. Other studies have shown that Runx1 induces the expression of RORγt, interacts with RORγt in conventional T cells, and regulates *Il17* transcription via controlling the promoter or enhancer regions of the *Il17* gene (Zhang et al., 2008). Runx3 also acts with T-bet to activate *Ifng* and silence *Il4* via binding to the *Ifng* promoter and the *Il4* silencer regions, respectively, leading to Th1 cell-specific cytokine production (Djuretic et al., 2007). Further, Runx1 and Runx3 interact with the *Cd4* silencer and the *Zbtb7b* silencer, in regulating thymocyte commitment to the CD8$^+$ T cell lineage by repressing the alternative cell fate (Setoguchi et al., 2008; Taniuchi et al., 2002). Thus, the Runx complex plays critical roles not only in T cell differentiation, in particular CD4-CD8 lineage commitment, but also in conferring a variety of functions to T cell subsets including Th1, Th17, and Treg cell. Further, phenotypical differences between *Runx1*- and *Runx3*-deleted Treg cells suggest that Runx1 and Runx3 differently contribute to the differentiation and the functions of T cell subsets. The Runx complex may thus function as an essential core transcriptional "modifier" to regulate specialized effector functions of CD4$^+$ T cell subsets by associating with particular lineage-specific transcription factors including FoxP3.

Regarding the mechanism by which Treg cell function is impaired in Cbfβ- or Runx1-deficient Treg cells, a notable finding is that Cbfβ or Runx1 deficiency accompanies attenuated expression of FoxP3 at mRNA and protein levels. Because attenuated FoxP3 expression can lead to loss of Treg cell-suppressive function, as demonstrated by others (Wan and Flavell, 2007), reduced expression of FoxP3 might be responsible for dysfunction of *Cbfb*-deleted Treg cells. For example, *Nrp1* and *Pde3b*, which were differentially expressed in *Cbfb*-deleted Treg cells by expression microarray, could be affected by FoxP3 hypoexpression. Other differentially expressed genes are also possibly associated with the impaired function of *Cbfb*-deleted Treg cells. They include *Il4*, *Ltb4r1*, *Cd160*, and *Ccr5*, all of which were overexpressed in *Cbfb*-deleted Treg cells. Of particular note is the hyperproduction of IL-4 by *Cbfb*-deleted Treg cells. Elevated IL-4 may contribute to the impaired Treg cell-mediated suppression in *Cbfb*- or *Runx1*-deleted Treg

cells because it has been shown that the addition of exogenous IL-4 renders $CD4^+CD25^-$ conventional T cells resistant to in vitro Treg cell-mediated suppression (Pace et al., 2006). We and others have previously reported that the Runx complex represses *Il4* via binding to the *Il4* silencer in naive $CD4^+$ T cells and Th1 cells (Djuretic et al., 2007; Naoe et al., 2007). Our observation that the Runx complex bound to the *Il4* silencer in Treg cells suggests that the complex similarly represses *Il4* expression in Treg cells and that loss of Runx complex derepresses *Il4*, leading to hyperproduction of IL-4 in *Cbfb*-deleted Treg cells. Nonetheless, it is also possible that reduction of FoxP3 expression directly derepresses *Il4* expression. Taken together, our findings show that impaired suppressive function of *Cbfb*-deleted Treg cells could be attributed, at least in part, to the reduction of FoxP3 and the hyperproduction of IL-4, in addition to the impaired formation of the Runx-Cbfβ-FoxP3 complex (Ono et al., 2007).

The maintenance of constitutive FoxP3 expression in Treg cells appears to require the Runx complex. Our observations that the complex bound to the regulatory regions of the *Foxp3* gene in Treg cells may suggest that the Runx complex would directly upregulate FoxP3 expression. In the reporter assays, however, Runx-binding site-dependent transactivation was observed only under activated condition, and not under unstimulated condition. This suggests that the Runx complex regulates constitutive FoxP3 expression more than by transactivating the *FOXP3* gene. It has also been shown that RUNX1 not only is a conventional transcriptional activator but also plays a critical role in chromatin modifications such as histone acetylation via interacting with histone acetyltransferases (Yoshida and Kitabayashi, 2008). This suggests that the binding of the Runx complex to the *Foxp3* gene regulatory regions may contribute to constitutive FoxP3 expression through epigenetic regulation. It is also possible that the deficiency of the Runx complex may primarily dysregulate other genes encoding molecules necessary for the maintenance of FoxP3 expression in Treg cells. These possibilities are currently under investigation.

Our results support the concept that Runx-dependent program plays essential roles for immune homeostasis including Treg cell-mediated immune suppression. Single-nucleotide polymorphisms (SNPs) affecting the consensus sites for RUNX1 are associated with the genetic susceptibility to several autoimmune diseases including systemic lupus erythematosus, rheumatoid arthritis, and psoriasis (Alarcon-Riquelme, 2004; Helms et al., 2003; Prokunina et al., 2002; Tokuhiro et al., 2003). In addition, a SNP in the *RUNX1* gene itself was strongly associated with rheumatoid arthritis (Tokuhiro et al., 2003). It is thus likely that genetic alterations of *RUNX1* may contribute to the development of autoimmune diseases in part by means of affecting Treg cell-mediated immune regulation. Furthermore, our study suggests that Treg cell-specific inhibition of the activity of the Runx1-Cbfβ complex could be useful for reducing Treg cell activity and thereby evoking effective tumor immunity.

EXPERIMENTAL PROCEDURES

Mice

C.B-17 SCID mice were purchased from CLEA Japan (Tokyo, Japan). BALB/c mice were purchased from Japan SLC (Shizuoka, Japan). *Foxp3-Ires-Cre (FIC)*, $Runx1^F$, $Runx3^F$, and $Cbfb^F$ mouse strains were described previously (Naoe et al., 2007; Taniuchi et al., 2002; Wing et al., 2008). In this paper, a mouse described with a "*FIC*" genotype was either a *FIC/Y* hemizygote male or *FIC/FIC* homozygote female. All mice were maintained in our animal facility and treated in accordance with the guidelines for animal care approved by the Institute for Frontier Medical Sciences, Kyoto University.

Antibodies

Biotinylated or FITC-, phycoerythrin (PE)-, PerCP-Cy5.5-, or allophycocyanin (APC)-conjugated mAbs for CD4, CD8, CD25, HSA (CD24), TCRβ, CD69, CD122, CD44, CD62L, CTLA-4, Ki-67, CD127, CD103, IFN-γ, IL-2, IL-4, IL-10, and IL-17 were purchased from BD Biosciences. Biotinylated anti-GITR (DTA1) was previously described (Shimizu et al., 2002). APC-conjugated anti-mouse Foxp3 (FJK-16 s) was purchased from eBioscience. The following mAbs were used for detecting human antigens: PerCP-Cy5.5-conjugated anti-CD4 and FITC-conjugated anti-CD45RO from BD Biosciences and biotinylated anti-human FOXP3 (236A/E7) from eBiosciences. Cbfβ antibody was generated by immunizing rabbits with peptides corresponding to the N-terminal of Cbfβ.

Histology

Gastritis and colitis were graded in a blinded fashion in accordance with the published criteria (Asano et al., 1996; Asseman et al., 1999).

Immunoblotting

Lysates prepared from purified 5×10^3 cells were loaded and immunoblotted with anti-Cbfβ.

Identification of $Cbfb^F$ and *Cbfb*-Deleted Allele by PCR

Equivalent amounts of genomic DNA extracted from individual lymphocyte subset were subjected to multiplex PCR with the following primers: G2, 5′-CCTCCTCATTCTAACAGGAATC-3′; G3, 5′-GGTTAGGAGTCATTGTGATC AC-3′; and G6, 5′-CATTGGATTGGCGTTACTGG-3′. $Cbfb^F$ and *Cbfb*-deleted alleles were identified by PCR amplification with the G3/G2 and the G3/G6 primer pair, respectively (Figure S13). The $Cbfb^F$ allele-specific and the *Cbfb*-deleted allele-specific amplicons were distinguished according to their length.

ELISA

Autoantibodies specific for gastric parietal cells were detected by ELISA as previously described (Sakaguchi et al., 1995). Serum IgG and IgE levels were assessed by ELISA with Mouse IgG ELISA Quantitation Kit (Bethyl Laboratories) and OptEIA Mouse IgE ELISA set (BD Biosciences), respectively.

Cell Sorting

Fresh mouse $CD4^+$ T cells were isolated as previously described (Hori et al., 2003). Then, $CD4^+$ T cell subpopulations including $CD4^+CD25^{hi}$ cells, $CD4^+CD25^-$ cells, and $CD4^+CD25^-CD45RB^{hi}$ cells were purified by sorting with a cell sorter (MoFlo, Dako). In some experiments, $CD4^+CD25^+$ cells were purified by MACS (Miltenyi Biotec).

Intracellular Cytokine Staining

Cells were stimulated for 5 hr with 20 ng/ml phorbol 12-myristate 13-acetate (PMA) and 1 μM ionomycin in the presence of GolgiStop (BD Biosciences). For intracellular cytokine staining, stimulated cells were stained for surface antigens, fixed, permeabilized with BD Cytofix/Cytoperm (BD Biosciences), and stained by anti-cytokine. For costaining of intracellular cytokine and FoxP3, stimulated cells were stained for surface antigens, fixed, permeabilized with Foxp3 Fixation/Permeabilization Kit (eBioscience), and finally, costained with cytokine antibody and Foxp3 antibody.

Proliferation Assay and Suppression Assay

A total of 2×10^4 responder T cells were cultured with or without graded numbers of suppressor cells for 3 days in the presence of 4×10^4 antigen-presenting cells (mitomycin C-treated $Thy1.2^+$ cell-depleted BALB/c splenocytes) and 0.5 μg/ml CD3 antibody (145-2C11, BD Biosciences). [^{3}H]thymidine (1 μCi/well) was added during the last 8 hr of culture.

Quantitative Real-Time RT-PCR

Total RNA was prepared from cells of interest with RNeasy Mini Kit (QIAGEN). cDNA was synthesized from total RNA with SuperScript III reverse transcriptase and oligo$(dT)_{12-18}$ primer (Invitrogen). Quantitative real-time RT-PCR was performed with the LightCycler 480 System (Roche Applied Science) with QuantiTect SYBR Green PCR Kit (QIAGEN). Primer pairs used are listed in Table S4. All samples were run in triplicate and the data were normalized to *Hprt* mRNA expression.

Chromatin Immunoprecipitation and Tiling Array

Cells were crosslinked by the addition of one-tenth volume of fresh 11% formaldehyde solution for 10 min at room temperature. Cells were resuspended, lysed in lysis buffers, and sonicated for solubilization and shearing of crosslinked DNA. The cell extract was incubated overnight at 4°C with 100 μl of Dynal anti-rabbit IgG magnetic beads that had been preincubated with 10 μg of the Cbfβ antibody. Beads were washed five times with RIPA buffer and one time with TE containing 50 mM NaCl. Bound complexes were eluted from the beads by heating at 65°C with occasional vortexing, and crosslinking was reversed by overnight incubation at 65°C. Immunoprecipitated DNA and whole-cell extract DNA were then purified by treatment with RNaseA, proteinase K, and multiple phenol:chloroform:isoamyl alcohol extractions. For conventional ChIP assays, the precipitated DNA was subjected to PCR amplification. The primers used are as follows: FxCNS1-for, 5′-AGCCCTGT TATCTCATTGATAC-3′; FxCNS1-rev, 5′-GACCTCGCTCTTCTAATAATCC-3′; FxCNS2-for, 5′-CCCATACCCACACTTTTGACCTCTG-3′; FxCNS2-rev, 5′-GC ACTTGAAAATGAGATAACTGTTCA-3′; FxCNS3-for, 5′-CTGGCATCCAAGAA AGACA-3′; and FxCNS3-rev, 5′-GGCTTCATCGGCAACAA-3′. Primers for *Il4* silencer region and for the region at 1 kb upstream of *Zbtb7b* (*Th-POK*) exon Ia (UP1) were described previously (Naoe et al., 2007; Setoguchi et al., 2008). For a ChIP-on-chip experiment, purified DNA was amplified twice by LM-PCR in accordance with the manufacturer's protocol (Agilent). We used mouse promoter array and custom microarrays generated by Agilent that tiled through several loci via 60-nucleotide oligonucleotide probes. The probes, representing the forward strand, were spaced every 200 bases and were printed at random location on the array. Probe hybridization and scanning of oligonucleotide array data were performed in accordance with the manufacturer's protocol (Agilent). Data analyses were carried out with Feature Extraction software and ChIP Analytics software (Agilent).

RNA Interference

MT-2 cells and MACS-sorted primary human $CD4^+$ T cells were transduced with *RUNX1* siRNA (HSS141472; Invitrogen) or Stealth RNAi negative control GC high (Invitrogen) as previously described (Ono et al., 2007).

Expression Microarray

Total RNA was isolated with the RNeasy Micro Kit (QIAGEN). Biotinylated antisense cRNA was prepared by two cycles of in vitro amplication. Biotinylated cRNA (15 μg) was hybridized to Affymetrix GeneChip Mouse Genome 430 2.0 arrays. Data analyses were done with the use of MeV (v4.2) (Saeed et al., 2003).

Induction of FoxP3 Expression in Human Naive T Cells

$CD25^-CD45RO^-$ primary human naive T cells were negatively sorted with MACS Pan T Cell Isolation Kit II, CD25 MicroBeads, and CD45RO MicroBeads (Miltenyi Biotec). A total of 7×10^6 purified naive T cells were transduced with control or *RUNX1* siRNA with a Human T Cell Nucleofector Kit (Amaxa), mixed with 4×10^6 T cell-depleted syngeneic PBMCs, and then cultured in a volume of 1 ml (12-well plates) for 24 h. Then, 7×10^5 cells were harvested and cultured in a volume of 200 μl (96-well plates) in the presence of 0.01 μg/ml anti-CD3 (OKT3) and 0.02 μg/ml anti-CD28 (CD28.2) for 4 days. Blood samples were obtained from healthy adult volunteers (20–40 years old). The study was conducted with the approval from the human ethics committee of the Institute for Frontier Medical Sciences, Kyoto University.

Statistical analysis

Comparisons were analyzed for statistical significance by Mann-Whitney U test, unless otherwise stated, with $p < 0.05$ being considered significant.

ACCESSION NUMBERS

Microarray data are available from the National Center for Biotechnology Information Gene Expression Omnibus (GEO) under accession number GSE18148.

SUPPLEMENTAL DATA

Supplemental Data include 13 figures, 5 tables, and Supplemental Experimental Procedures and can be found with this article online at http://www.cell.com/immunity/supplemental/S1074-7613(09)00407-5.

ACKNOWLEDGMENTS

We thank M. Kakino, R. Ishii, M. Yoshida, and K. Akiyama for technical assistance; M. Matsuoka for ATL-43T cell line; and M. Matsushita for preparing histology.

Received: August 24, 2009
Revised: September 9, 2009
Accepted: September 14, 2009
Published online: October 1, 2009

REFERENCES

Alarcon-Riquelme, M.E. (2004). Role of RUNX in autoimmune diseases linking rheumatoid arthritis, psoriasis and lupus. Arthritis Res. Ther. *6*, 169–173.

Annacker, O., Coombes, J.L., Malmstrom, V., Uhlig, H.H., Bourne, T., Johansson-Lindbom, B., Agace, W.W., Parker, C.M., and Powrie, F. (2005). Essential role for CD103 in the T cell-mediated regulation of experimental colitis. J. Exp. Med. *202*, 1051–1061.

Asano, M., Toda, M., Sakaguchi, N., and Sakaguchi, S. (1996). Autoimmune disease as a consequence of developmental abnormality of a T cell subpopulation. J. Exp. Med. *184*, 387–396.

Asseman, C., Mauze, S., Leach, M.W., Coffman, R.L., and Powrie, F. (1999). An essential role for interleukin 10 in the function of regulatory T cells that inhibit intestinal inflammation. J. Exp. Med. *190*, 995–1004.

Bettelli, E., Dastrange, M., and Oukka, M. (2005). Foxp3 interacts with nuclear factor of activated T cells and NF-kappa B to repress cytokine gene expression and effector functions of T helper cells. Proc. Natl. Acad. Sci. USA *102*, 5138–5143.

Cao, X., Cai, S.F., Fehniger, T.A., Song, J., Collins, L.I., Piwnica-Worms, D.R., and Ley, T.J. (2007). Granzyme B and perforin are important for regulatory T cell-mediated suppression of tumor clearance. Immunity *27*, 635–646.

de Bruijn, M.F., and Speck, N.A. (2004). Core-binding factors in hematopoiesis and immune function. Oncogene *23*, 4238–4248.

Djuretic, I.M., Levanon, D., Negreanu, V., Groner, Y., Rao, A., and Ansel, K.M. (2007). Transcription factors T-bet and Runx3 cooperate to activate Ifng and silence Il4 in T helper type 1 cells. Nat. Immunol. *8*, 145–153.

Durst, K.L., and Hiebert, S.W. (2004). Role of RUNX family members in transcriptional repression and gene silencing. Oncogene *23*, 4220–4224.

Egawa, T., Tillman, R.E., Naoe, Y., Taniuchi, I., and Littman, D.R. (2007). The role of the Runx transcription factors in thymocyte differentiation and in homeostasis of naive T cells. J. Exp. Med. *204*, 1945–1957.

Fontenot, J.D., Gavin, M.A., and Rudensky, A.Y. (2003). Foxp3 programs the development and function of CD4+CD25+ regulatory T cells. Nat. Immunol. *4*, 330–336.

Gondek, D.C., Lu, L.F., Quezada, S.A., Sakaguchi, S., and Noelle, R.J. (2005). Cutting edge: Contact-mediated suppression by CD4+CD25+ regulatory cells involves a granzyme B-dependent, perforin-independent mechanism. J. Immunol. *174*, 1783–1786.

Grueter, B., Petter, M., Egawa, T., Laule-Kilian, K., Aldrian, C.J., Wuerch, A., Ludwig, Y., Fukuyama, H., Wardemann, H., Waldschuetz, R., et al. (2005). Runx3 regulates integrin alpha E/CD103 and CD4 expression during development of CD4-/CD8+ T cells. J. Immunol. *175*, 1694–1705.

Helms, C., Cao, L., Krueger, J.G., Wijsman, E.M., Chamian, F., Gordon, D., Heffernan, M., Daw, J.A., Robarge, J., Ott, J., et al. (2003). A putative RUNX1 binding site variant between SLC9A3R1 and NAT9 is associated with susceptibility to psoriasis. Nat. Genet. *35*, 349–356.

Hill, J.A., Feuerer, M., Tash, K., Haxhinasto, S., Perez, J., Melamed, R., Mathis, D., and Benoist, C. (2007). Foxp3 transcription-factor-dependent and -independent regulation of the regulatory T cell transcriptional signature. Immunity *27*, 786–800.

Hori, S., Nomura, T., and Sakaguchi, S. (2003). Control of regulatory T cell development by the transcription factor Foxp3. Science *299*, 1057–1061.

Khattri, R., Cox, T., Yasayko, S.A., and Ramsdell, F. (2003). An essential role for Scurfin in CD4+CD25+ T regulatory cells. Nat. Immunol. *4*, 337–342.

Kim, H.P., and Leonard, W.J. (2007). CREB/ATF-dependent T cell receptor-induced FoxP3 gene expression: A role for DNA methylation. J. Exp. Med. *204*, 1543–1551.

Komine, O., Hayashi, K., Natsume, W., Watanabe, T., Seki, Y., Seki, N., Yagi, R., Sukzuki, W., Tamauchi, H., Hozumi, K., et al. (2003). The Runx1 transcription factor inhibits the differentiation of naive CD4+ T cells into the Th2 lineage by repressing GATA3 expression. J. Exp. Med. *198*, 51–61.

Li, B., Samanta, A., Song, X., Iacono, K.T., Bembas, K., Tao, R., Basu, S., Riley, J.L., Hancock, W.W., Shen, Y., et al. (2007). FOXP3 interactions with histone acetyltransferase and class II histone deacetylases are required for repression. Proc. Natl. Acad. Sci. USA *104*, 4571–4576.

Mantel, P.Y., Ouaked, N., Ruckert, B., Karagiannidis, C., Welz, R., Blaser, K., and Schmidt-Weber, C.B. (2006). Molecular mechanisms underlying FOXP3 induction in human T cells. J. Immunol. *176*, 3593–3602.

Naoe, Y., Setoguchi, R., Akiyama, K., Muroi, S., Kuroda, M., Hatam, F., Littman, D.R., and Taniuchi, I. (2007). Repression of interleukin-4 in T helper type 1 cells by Runx/Cbf beta binding to the Il4 silencer. J. Exp. Med. *204*, 1749–1755.

Ochs, H.D., Ziegler, S.F., and Torgerson, T.R. (2005). FOXP3 acts as a rheostat of the immune response. Immunol. Rev. *203*, 156–164.

Ono, M., Yaguchi, H., Ohkura, N., Kitabayashi, I., Nagamura, Y., Nomura, T., Miyachi, Y., Tsukada, T., and Sakaguchi, S. (2007). Foxp3 controls regulatory T-cell function by interacting with AML1/Runx1. Nature *446*, 685–689.

Pace, L., Rizzo, S., Palombi, C., Brombacher, F., and Doria, G. (2006). Cutting edge: IL-4-induced protection of CD4+CD25- Th cells from CD4+CD25+ regulatory T cell-mediated suppression. J. Immunol. *176*, 3900–3904.

Prokunina, L., Castillejo-Lopez, C., Oberg, F., Gunnarsson, I., Berg, L., Magnusson, V., Brookes, A.J., Tentler, D., Kristjansdottir, H., Grondal, G., et al. (2002). A regulatory polymorphism in PDCD1 is associated with susceptibility to systemic lupus erythematosus in humans. Nat. Genet. *32*, 666–669.

Saeed, A.I., Sharov, V., White, J., Li, J., Liang, W., Bhagabati, N., Braisted, J., Klapa, M., Currier, T., Thiagarajan, M., et al. (2003). TM4: A free, open-source system for microarray data management and analysis. Biotechniques *34*, 374–378.

Sakaguchi, S., Ono, M., Setoguchi, R., Yagi, H., Hori, S., Fehervari, Z., Shimizu, J., Takahashi, T., and Nomura, T. (2006). Foxp3+ CD25+ CD4+ natural regulatory T cells in dominant self-tolerance and autoimmune disease. Immunol. Rev. *212*, 8–27.

Sakaguchi, S., Sakaguchi, N., Asano, M., Itoh, M., and Toda, M. (1995). Immunologic self-tolerance maintained by activated T cells expressing IL-2 receptor alpha-chains (CD25). Breakdown of a single mechanism of self-tolerance causes various autoimmune diseases. J. Immunol. *155*, 1151–1164.

Sato, T., Ohno, S., Hayashi, T., Sato, C., Kohu, K., Satake, M., and Habu, S. (2005). Dual functions of Runx proteins for reactivating CD8 and silencing CD4 at the commitment process into CD8 thymocytes. Immunity *22*, 317–328.

Setoguchi, R., Tachibana, M., Naoe, Y., Muroi, S., Akiyama, K., Tezuka, C., Okuda, T., and Taniuchi, I. (2008). Repression of the transcription factor Th-POK by Runx complexes in cytotoxic T cell development. Science *319*, 822–825.

Shimizu, J., Yamazaki, S., Takahashi, T., Ishida, Y., and Sakaguchi, S. (2002). Stimulation of CD25(+)CD4(+) regulatory T cells through GITR breaks immunological self-tolerance. Nat. Immunol. *3*, 135–142.

Speck, N.A. (2001). Core binding factor and its role in normal hematopoietic development. Curr. Opin. Hematol. *8*, 192–196.

Taniuchi, I., and Littman, D.R. (2004). Epigenetic gene silencing by Runx proteins. Oncogene *23*, 4341–4345.

Taniuchi, I., Osato, M., Egawa, T., Sunshine, M.J., Bae, S.C., Komori, T., Ito, Y., and Littman, D.R. (2002). Differential requirements for Runx proteins in CD4 repression and epigenetic silencing during T lymphocyte development. Cell *111*, 621–633.

Tokuhiro, S., Yamada, R., Chang, X., Suzuki, A., Kochi, Y., Sawada, T., Suzuki, M., Nagasaki, M., Ohtsuki, M., Ono, M., et al. (2003). An intronic SNP in a RUNX1 binding site of SLC22A4, encoding an organic cation transporter, is associated with rheumatoid arthritis. Nat. Genet. *35*, 341–348.

Tone, Y., Furuuchi, K., Kojima, Y., Tykocinski, M.L., Greene, M.I., and Tone, M. (2008). Smad3 and NFAT cooperate to induce Foxp3 expression through its enhancer. Nat. Immunol. *9*, 194–202.

van Wijnen, A.J., Stein, G.S., Gergen, J.P., Groner, Y., Hiebert, S.W., Ito, Y., Liu, P., Neil, J.C., Ohki, M., and Speck, N. (2004). Nomenclature for Runt-related (RUNX) proteins. Oncogene *23*, 4209–4210.

Walker, M.R., Kasprowicz, D.J., Gersuk, V.H., Benard, A., Van Landeghen, M., Buckner, J.H., and Ziegler, S.F. (2003). Induction of FoxP3 and acquisition of T regulatory activity by stimulated human CD4+CD25- T cells. J. Clin. Invest. *112*, 1437–1443.

Wan, Y.Y., and Flavell, R.A. (2007). Regulatory T-cell functions are subverted and converted owing to attenuated Foxp3 expression. Nature *445*, 766–770.

Wing, K., Onishi, Y., Prieto-Martin, P., Yamaguchi, T., Miyara, M., Fehervari, Z., Nomura, T., and Sakaguchi, S. (2008). CTLA-4 control over Foxp3+ regulatory T cell function. Science *322*, 271–275.

Woolf, E., Xiao, C., Fainaru, O., Lotem, J., Rosen, D., Negreanu, V., Bernstein, Y., Goldenberg, D., Brenner, O., Berke, G., et al. (2003). Runx3 and Runx1 are required for CD8 T cell development during thymopoiesis. Proc. Natl. Acad. Sci. USA *100*, 7731–7736.

Wu, Y., Borde, M., Heissmeyer, V., Feuerer, M., Lapan, A.D., Stroud, J.C., Bates, D.L., Guo, L., Han, A., Ziegler, S.F., et al. (2006). FOXP3 controls regulatory T cell function through cooperation with NFAT. Cell *126*, 375–387.

Yoshida, H., and Kitabayashi, I. (2008). Chromatin regulation by AML1 complex. Int. J. Hematol. *87*, 19–24.

Zhang, F., Meng, G., and Strober, W. (2008). Interactions among the transcription factors Runx1, RORgammat and Foxp3 regulate the differentiation of interleukin 17-producing T cells. Nat. Immunol. *9*, 1297–1306.

copy number in TG of GrB$^{-/-}$ or Pfn$^{-/-}$ mice. This mechanism might be particularly efficient during attempted HSV-1 reactivation events where ICP4 expression has escaped repression by viral miRNAs and host neuron epigenetic modifications. Thus, we propose a tripartite relation in which HSV-1 latency is maintained through the activity of the virus, host neuron, and contiguous CD8$^+$ T cells permitting viral persistence with neuronal survival (fig. S7).

References and Notes

1. D. Theil *et al.*, *Am. J. Pathol.* **163**, 2179 (2003).
2. K. Hufner *et al.*, *J. Neuropathol. Exp. Neurol.* **65**, 1022 (2006).
3. G. M. Verjans *et al.*, *Proc. Natl. Acad. Sci. U.S.A.* **104**, 3496 (2007).
4. T. Derfuss *et al.*, *Brain Pathol.* **17**, 389 (2007).
5. A. Simmons, D. C. Tscharke, *J. Exp. Med.* **175**, 1337 (1992).
6. E. M. Cantin, D. R. Hinton, J. Chen, H. Openshaw, *J. Virol.* **69**, 4898 (1995).
7. C. Shimeld *et al.*, *J. Neuroimmunol.* **61**, 7 (1995).
8. T. Liu, Q. Tang, R. L. Hendricks, *J. Virol.* **70**, 264 (1996).
9. K. M. Khanna, R. H. Bonneau, P. R. Kinchington, R. L. Hendricks, *Immunity* **18**, 593 (2003).
10. T. Liu *et al.*, *J. Exp. Med.* **191**, 1459 (2000).
11. M. L. Freeman, B. S. Sheridan, R. H. Bonneau, R. L. Hendricks, *J. Immunol.* **179**, 322 (2007).
12. K. D. Croen *et al.*, *N. Engl. J. Med.* **317**, 1427 (1987).
13. W. G. Stroop, D. C. Schaefer, *Acta Neuropathol.* **74**, 124 (1987).
14. T. Liu, K. M. Khanna, B. N. Carriere, R. L. Hendricks, *J. Virol.* **75**, 11178 (2001).
15. V. Decman, P. R. Kinchington, S. A. Harvey, R. L. Hendricks, *J. Virol.* **79**, 10339 (2005).
16. Materials and methods are available as supporting material on *Science* Online.
17. W. G. Telford, A. Komoriya, B. Z. Packard, *Cytometry* **47**, 81 (2002).
18. G.-C. Perng *et al.*, *Science* **287**, 1500 (2000).
19. Y. Hoshino, L. Pesnicak, J. I. Cohen, S. E. Straus, *J. Virol.* **81**, 8157 (2007).
20. R. A. Pereira, M. M. Simon, A. Simmons, *J. Virol.* **74**, 1029 (2000).
21. F. Andrade *et al.*, *EMBO J.* **26**, 2148 (2007).
22. C. Backes *et al.*, *Nucleic Acids Res.* **33**, W208 (2005).
23. N. A. DeLuca, A. M. McCarthy, P. A. Schaffer, *J. Virol.* **56**, 558 (1985).
24. J. L. Umbach *et al.*, *Nature* **454**, 780 (2008).
25. D. M. Knipe, A. Cliffe, *Nat. Rev. Microbiol.* **6**, 211 (2008).
26. B. S. Sheridan, J. E. Knickelbein, R. L. Hendricks, *Expert Opin. Biol. Ther.* **7**, 1323 (2007).
27. S. N. Mueller *et al.*, *J. Virol.* **77**, 2445 (2003).

28. We thank K. Lathrop and J. Karlsson for assistance with microscopy and preparation of figures and N. Zurowski for assistance with flow cytometry. We have no conflicting financial interests. This work was supported by NIH grants F30NS061471 (J.E.K.), R01EY05945 (R.L.H.), R01EY015291 (P.R.K.), and P30EY08098 (R.L.H.); a Research to Prevent Blindness Medical Student Eye Research Fellowship (J.E.K.); and unrestricted grants from Research to Prevent Blindness and the Eye and Ear Foundation of Pittsburgh (R.L.H.).

Supporting Online Material

www.sciencemag.org/cgi/content/full/322/5899/268/DC1
Materials and Methods
Figs. S1 to S7
References

4 August 2008; accepted 11 September 2008
10.1126/science.1164164

CTLA-4 Control over Foxp3$^+$ Regulatory T Cell Function

Kajsa Wing,[1]* Yasushi Onishi,[1,2] Paz Prieto-Martin,[1] Tomoyuki Yamaguchi,[1] Makoto Miyara,[1] Zoltan Fehervari,[1] Takashi Nomura,[1] Shimon Sakaguchi[1,3,4]†

Naturally occurring Foxp3$^+$CD4$^+$ regulatory T cells (Tregs) are essential for maintaining immunological self-tolerance and immune homeostasis. Here, we show that a specific deficiency of cytotoxic T lymphocyte antigen 4 (CTLA-4) in Tregs results in spontaneous development of systemic lymphoproliferation, fatal T cell–mediated autoimmune disease, and hyperproduction of immunoglobulin E in mice, and it also produces potent tumor immunity. Treg-specific CTLA-4 deficiency impairs in vivo and in vitro suppressive function of Tregs—in particular, Treg-mediated down-regulation of CD80 and CD86 expression on dendritic cells. Thus, natural Tregs may critically require CTLA-4 to suppress immune responses by affecting the potency of antigen-presenting cells to activate other T cells.

Naturally occurring CD25$^+$CD4$^+$ regulatory T cells (Tregs), which specifically express the transcription factor Foxp3, suppress aberrant immune responses, including autoimmune diseases and allergy (*1*). Furthermore, reduction or expansion of Tregs can be exploited to provoke effective tumor immunity or transplantation tolerance, respectively. Two cardinal features of Foxp3$^+$ Tregs are that they constitutively express cytotoxic T lymphocyte antigen 4 (CTLA-4), which only happens after activation in other T cell subsets (*2*–*4*), and that Foxp3 controls the expression of CTLA-4 in Tregs (*5*–*9*). CTLA-4 is a potent negative regulator of T cell immune responses, as illustrated by CTLA-4 knockout (KO) mice, which die prematurely from multiorgan inflammation (*10*, *11*). The polymorphism of the CTLA-4 gene contributes substantially to the genetic susceptibility to autoimmune diseases such as type 1 diabetes (*12*). Moreover, autoimmunity, inflammatory bowel disease, and tumor immunity can be elicited by blocking CTLA-4 with a specific antibody (*3*, *4*, *13*–*15*). Yet the manner in which CTLA-4 negatively controls immune responses is controversial (*16*). CTLA-4 expressed by activated effector T cells may mediate a negative signal that attenuates their activation. Alternatively, but not exclusively, Foxp3$^+$ Tregs may require CTLA-4 for their suppressive function. By specifically deleting the CTLA-4 gene in Foxp3$^+$ Tregs in mice, we have attempted to determine the role of CTLA-4 for the maintenance of self-tolerance and immune homeostasis.

We generated BALB/c mice expressing Cre under the control of the Foxp3 promoter—hereafter called FIC (Fox-IRES-Cre) mice—and BALB/c mice expressing a floxed CTLA-4 gene (CTLA-4$^{fl/fl}$) [supporting online material (SOM) text and fig. S1] (*17*). Compared with BALB/c wild-type (WT) mice, FIC mice expressed Foxp3 protein at slightly lower levels whereas CTLA-4$^{fl/fl}$ mice expressed equivalent levels of CTLA-4 (Fig. 1A). To assess the specificity of Cre expression, FIC mice were crossed with Cre reporter mice (CAG mice), which express enhanced green fluorescent protein (EGFP) only in Cre$^+$ cells (*18*). EGFP expression was confined to ~15% of CD4$^+$ T cells and ~1.5% of CD8$^+$ T cells (Fig. 1B). The vast majority of EGFP$^+$CD4$^+$ T cells in adult FIC$^{+/+}$ CAG mice were Foxp3$^+$ (97.1 ± 1.2%, $n = 4$ mice), indicating that Foxp3 expression is stable once the gene is turned on and Cre expression is not leaky in Foxp3$^-$ cells (Fig. 1C). On the basis of this specific expression of Cre in Foxp3$^+$ Tregs, we generated CTLA-4 conditional KO (CKO) mice by crossing FIC and CTLA-4$^{fl/fl}$ mice. CTLA-4 was specifically deleted in CD4$^+$Foxp3$^+$ T cells, as compared with FIC$^{+/+}$ WT or full CTLA-4 KO mice (Fig. 1D). CKO mice even harbored a higher frequency of CTLA-4–expressing CD4$^+$Foxp3$^-$ cells than did WT littermates (Fig. 1E). Whereas KO mice became moribund at ~20 days of age (*10*, *11*), CKO mice remained apparently unaffected until ~7 weeks of age, when they rapidly became inactive and began to develop general edema that was frequently accompanied by ascites (Fig. 1F). Thus, CTLA-4 deficiency in Tregs alone suffices to cause fatal disease, whereas the additional CTLA-4 deficiency in non-Treg cells enhances the disease. Yet, CTLA-4 expression in activated effector T cells per se is insufficient to prevent it.

Pathological analysis of CKO mice revealed splenomegaly and lymphadenopathy, which was reflected in increased cell numbers (Fig. 2, A and B). The proportion of CD4$^+$ T cells was unaltered, whereas CD8$^+$ T cells were decreased (Fig. 2C). Cardiomegaly and congestion of the liver was macroscopically evident in the terminal stage of every case. In affected hearts, mononuclear cells densely infiltrated into the myocardium and destroyed myocytes (Fig. 2, D to G), indicating that the plausible cause of sudden death in CKO mice is

[1]Department of Experimental Pathology, Institute for Frontier Medical Sciences, Kyoto University, Kyoto 606-8507, Japan. [2]Department of Rheumatology and Haematology, Tohoku University Graduate School of Medicine, Sendai 980-8574, Japan. [3]Core Research for Evolutional Science and Technology, Japan Science and Technology Agency, Kawaguchi 332-0012, Japan. [4]Laboratory of Experimental Immunology, World Premier International Immunology Frontier Research Center, Osaka University, Suita 565-0871, Japan.

*Present address: Department of Medical Inflammation Research, Karolinska Institute, Stockholm 17177, Sweden.
†To whom correspondence should be addressed. E-mail: shimon@frontier.kyoto-u.ac.jp

heart failure due to severe myocarditis (*19*). In addition, CKO mice possessed focal lymphocyte infiltrations in lung and salivary gland and suffered from gastritis with various degrees of destruction of gastric parietal cells and chief cells. Antiparietal autoantibodies were readily detected in the sera of CKO mice and a proportion of $FIC^{+/+}$ mice, in which the lower expression of Foxp3 in Tregs (Fig. 1A) might somehow affect Treg function (*20*) (Fig. 2, H to N, and SOM text). Myocarditis and gastritis in CKO mice (and gastritis in FIC mice) could be adoptively transferred with splenocytes and purified $CD4^+$ T cells into T cell–deficient BALB/c athymic nude (nu/nu) mice, indicating that these autoimmune conditions were both T cell–mediated (Fig. 2O and fig. S2). Furthermore, CKO mice developed several hundred-fold and threefold higher levels of serum immunoglobulin E (IgE) and immunoglobulin G (IgG), respectively, than the levels in FIC or WT mice (Fig. 2, P and Q).

Costaining of intracellular cytokines and Foxp3 revealed an increased frequency of interleukin-2 (IL-2)–, IL-4–, and IFN-γ–producing $Foxp3^-CD4^+$ cells in both the spleen and lymph node (LN) of diseased CKO and KO mice (Fig. 2R and fig. S3). IL-17–secreting (Th17) cells increased in KO but not CKO mice, suggesting that Th17 cells might contribute to the rapid disease progression in the former. Thus, CTLA-4–deficient Tregs fail to control the spontaneous activation of other T cells and their differentiation into Th1 and Th2 lineage cells that mediate autoimmune disease and allergy.

We next tested whether Treg-specific CTLA-4 deficiency also influenced the potency of tumor immunity. BALB/c nu/nu mice were reconstituted with splenocytes from CKO or control FIC mice containing equivalent numbers of T cells and inoculated with BALB/c-derived RL♂1 leukemia cells (*21*). All recipients of FIC splenocytes died of tumor progression within a month. In contrast, recipients of CKO splenocytes halted the tumor growth, with the majority surviving the 6-week observation period, during which 60% of them completely rejected the tumor (Fig. 3A). As previously shown (*21*), transfer of BALB/c splenocytes after depletion of $CD25^+$ T cells led to the rejection of RL♂1 leukemia cells in nu/nu mice. In this setting, FIC Tregs cotransferred with $CD25^-$ T cells suppressed tumor rejection, whereas CKO Tregs did not (Fig. 3B). Thus, Treg-specific CTLA-4 deficiency affects in vivo Treg suppressive function, leading to enhanced tumor immunity.

We next explored the possibility that CTLA-4 deficiency might impair the generation, survival, or suppressive function of $Foxp3^+$ Tregs. CKO mice exhibited no significant alteration in number or composition of $CD4^+$ and $CD8^+$ thymocytes (Fig. 4A). The majority of $Foxp3^+$ WT thymocytes expressed CTLA-4, whereas $Foxp3^+$ CKO thymocytes contained a mix of $CTLA\text{-}4^+$ and $CTLA\text{-}4^-$ cells in both the CD4–single positive and CD4/CD8–double positive compartments (Fig. 4A). Because the CTLA-4 gene is deleted only after Foxp3 is expressed, CTLA-4 is either up-regulated before Foxp3 expression in CKO mice or it may take some time for the Cre protein to accumulate in $Foxp3^+$ cells, meanwhile allowing the expression of CTLA-4. The frequency of $Foxp3^+$ thymocytes was not significantly changed between CKO and WT mice, whereas the number of $Foxp3^+$ and $Foxp3^-$ T cells in the spleen and LNs increased enormously by active proliferation (Fig. 4B, figs. S4 and S5, and SOM text). Thus, Foxp3-inducible CTLA-4 deficiency minimally alters thymic selection of Tregs and probably triggers immunological diseases through affecting Treg function in the periphery.

Because Foxp3 is encoded by the X chromosome, female nonautoimmune $FIC^{+/-}CTLA\text{-}4^{fl/fl}$ mice are a mosaic for CTLA-4–intact and –deficient Tregs. They harbored equal numbers of $CTLA\text{-}4^+$ and $CTLA\text{-}4^-$ $Foxp3^+$ T cells, indicating that both populations equally survive in physiological non-inflammatory conditions (Fig. 4C). Furthermore, when CTLA-4–deficient or –intact Tregs were transferred to nu/nu mice, both populations showed a similar degree of homeostatic proliferation, and neither one caused autoimmunity (fig. S6). CTLA-4–deficient $Foxp3^+$ Tregs were as poor at producing pro-inflammatory cytokines as were their WT or FIC counterparts (fig. S3). Taken together, CTLA-4 deficiency, per se, does not affect the survival of Tregs or render them pathogenic.

Phenotypically, CTLA-4–deficient naive Tregs in $FIC^{+/-}CTLA\text{-}4^{fl/fl}$ females normally expressed typical Treg markers including CD44, CD103, glucocorticoid-induced tumor necrosis factor receptor, latency-associated peptide, and intracellular IL-10 (Fig. 4D and fig. S7). The comparatively higher expression of these molecules by Tregs from CKO mice is presumably secondary to ongoing inflammation in CKO mice, as illustrated by an activated phenotype of their $Foxp3^-$ non-Treg cells.

CTLA-4–deficient Tregs, whether naive from $FIC^{+/-}CTLA\text{-}4^{fl/fl}$ CAG females or activated from CKO mice, had diminished suppressive capacity compared with CTLA-4–intact Tregs in cultures of carboxyfluorescein diacetate succinimidyl ester (CFSE)–labeled responder T cells (Tresp) in the presence of splenic $CD11c^+$ dendritic cells (DCs) and anti-CD3 monoclonal antibody (mAb), as assessed by the percentage and number of CFSE-diluting (i.e., divided) Tresp (Fig. 4E, figs. S8 and S9, and SOM text). Moreover, CKO Tregs clearly failed to suppress allo-reactive Tresp proliferation, even at high Treg/Tresp ratios (Fig. 4F). FIC or WT Tregs, whether cultured alone or together with Tresp cells, specifically hampered up-regulation of the expression of CD80 and CD86, but not CD40 and major histocompatability complex class II, in DCs (*22–26*). In contrast, CKO Tregs failed to exert this effect (Fig. 4G, figs. S10 to S13, and SOM text). Activated FIC Tregs (but

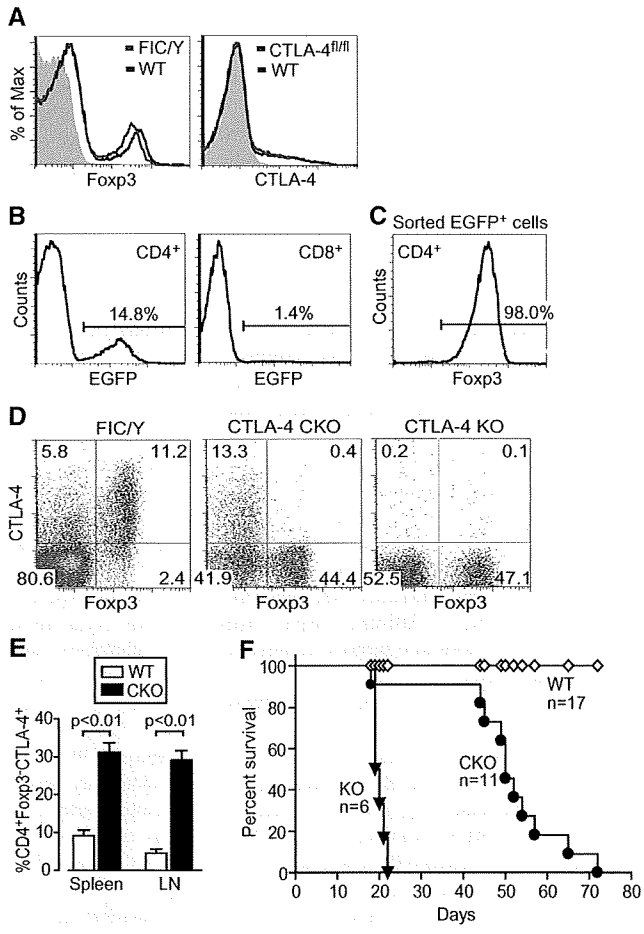

Fig. 1. Specific deletion of CTLA-4 expression in $Foxp3^+$ T cells results in fatal disease. **(A)** Flow cytometric analysis of intracellular Foxp3 (left) and CTLA-4 (right) in freshly isolated LN $CD4^+$ T cells from male FIC, $CTLA\text{-}4^{fl/fl}$, or BALB/c WT mice. **(B)** EGFP expression in $CD4^+$ or $CD8^+$ T cells derived from male FIC-CAG mice. **(C)** Sorted $CD4^+EGFP^+$ cells in FIC-CAG mice were stained for Foxp3. **(D)** CTLA-4 and Foxp3 expression in LN $CD4^+$ T cells from BALB/c WT, CKO, or KO mice. **(E)** Frequency of CTLA-4–expressing $CD4^+Foxp3^-$ T cells in CKO and normal littermates (n = 5). **(F)** Survival of KO and CKO mice as compared with normal littermates. Data represent three or more independent experiments. Vertical bars indicate SEM.

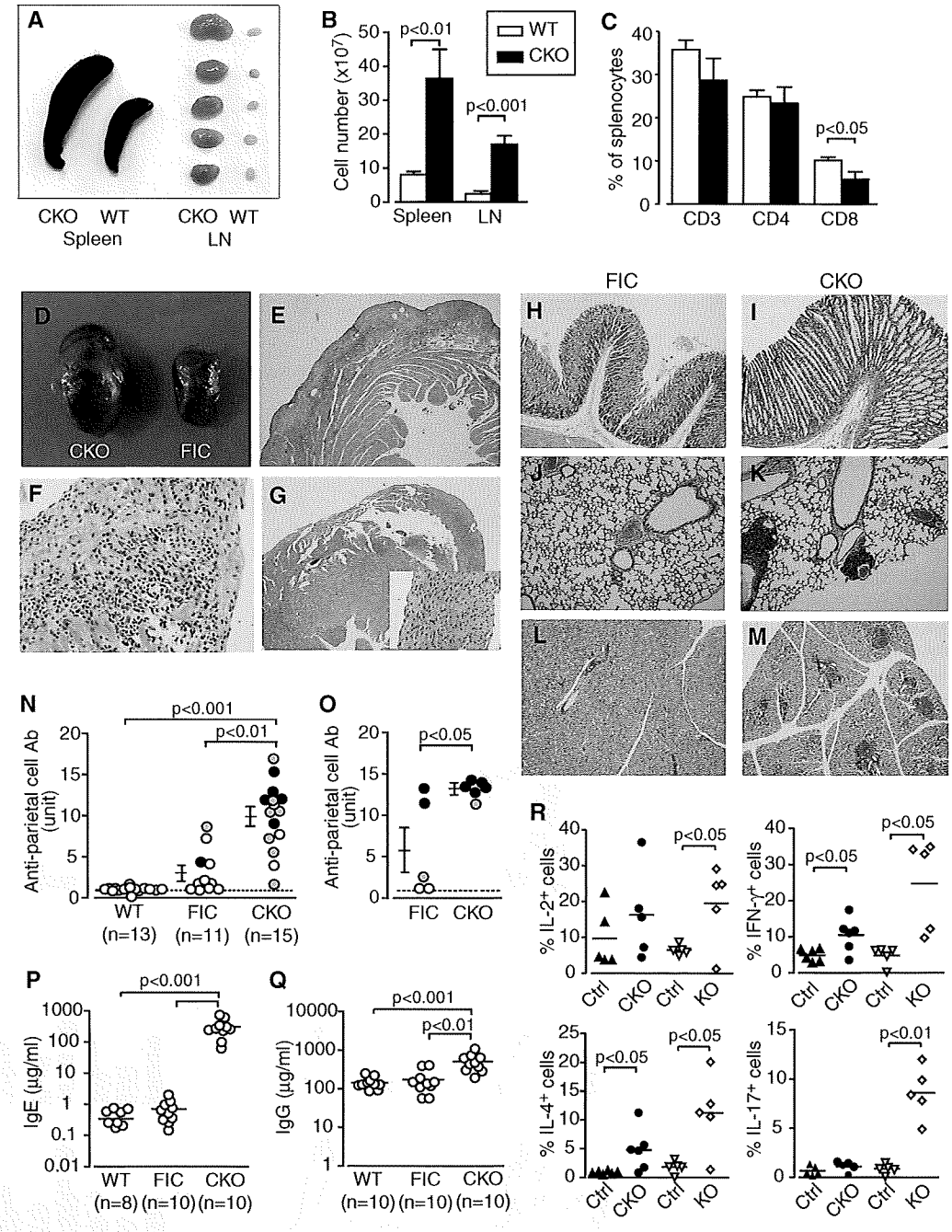

Fig. 2. Autoimmune disease and hyperproduction of IgE in CKO mice. (**A**) Splenomegaly and lymphadenopathy in a CKO and a WT littermate. Lymphocyte numbers (**B**) and frequencies of T cell subsets (**C**) in spleens of 6- to 10-week-old CKO and WT littermates (n = 11 to 13). (**D**) The heart of a CKO (left) and a FIC$^{+/-}$CTLA-4$^{fl/fl}$ mouse (right). Histology (hematoxylin and eosin staining) of the heart of a CKO [(**E** and **F**) ×50 and ×200, respectively] and a FIC mouse [(**G**) ×50; inset, ×200]. Histology of the stomach [(**H** and **I**) ×100], lung [(**J** and **K**) ×100], and salivary gland [(**L** and **M**) ×50] of a CKO [(H), (J), and (L)] and a FIC mouse [(I), (K), and (M)]. Serological and histological development of gastritis in WT, FIC$^{+/+}$, and CKO mice (**N**), and BALB/c nu/nu mice 7 weeks after cell transfer from CKO or FIC$^{+/+}$ mice (**O**). Gastric lesions were histologically graded as 2 (black circle), 1 (gray circle), and 0 (open circle) (*19*). Serum concentrations of IgE (**P**) and IgG (**Q**) in indicated groups of mice. (**R**) Frequencies of cytokine-producing cells among CD4$^+$Foxp3$^-$ splenocytes of 6- to 9-week-old CKO, 16- to 20-day-old KO, or normal littermates (n = 5 to 6). Error bars indicate SEM.

not activated CKO Tregs) also reduced the expression of CD86-GFP fusion protein retrovirally expressed in L-cells, a fibroblast cell line (Fig. 4H). This indicates that Treg-dependant modulation of CD86 expression on DCs is at least partly due to down-regulation of the expression and not masking of the molecule by soluble CTLA-4. Taken together, Treg-mediated CD80/CD86 down-regulation may limit the activation of naive T cells via CD28, resulting in specific immune suppression and tolerance.

Thus, CTLA-4 expressed in Foxp3$^+$ Tregs is critically required for their in vivo and in vitro suppression, which is mediated at least in part by

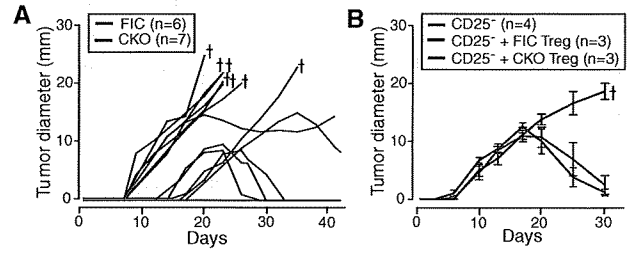

Fig. 3. Treg-specific CTLA-4 deficiency promotes tumor immunity. (**A**) BALB/c nu/nu mice received 3 × 10^7 splenocytes from FIC or CKO mice, followed by intradermal inoculation of 1.5 × 10^5 RLσ1 leukemia cells. Crosses indicate death due to tumor growth. (**B**) BALB/c CD25$^-$ cells (1.5 × 10^7) were cotransferred with 3.8 × 10^5 CD25^{high}CD4$^+$ T cells from CKO or FIC mice and inoculated with 1.5 × 10^5 RLσ1 cells (n = 3). Tumor diameters were measured every other day for 6 weeks. Mice were euthanized when tumor diameters exceeded 20 mm. Error bars indicate SEM.

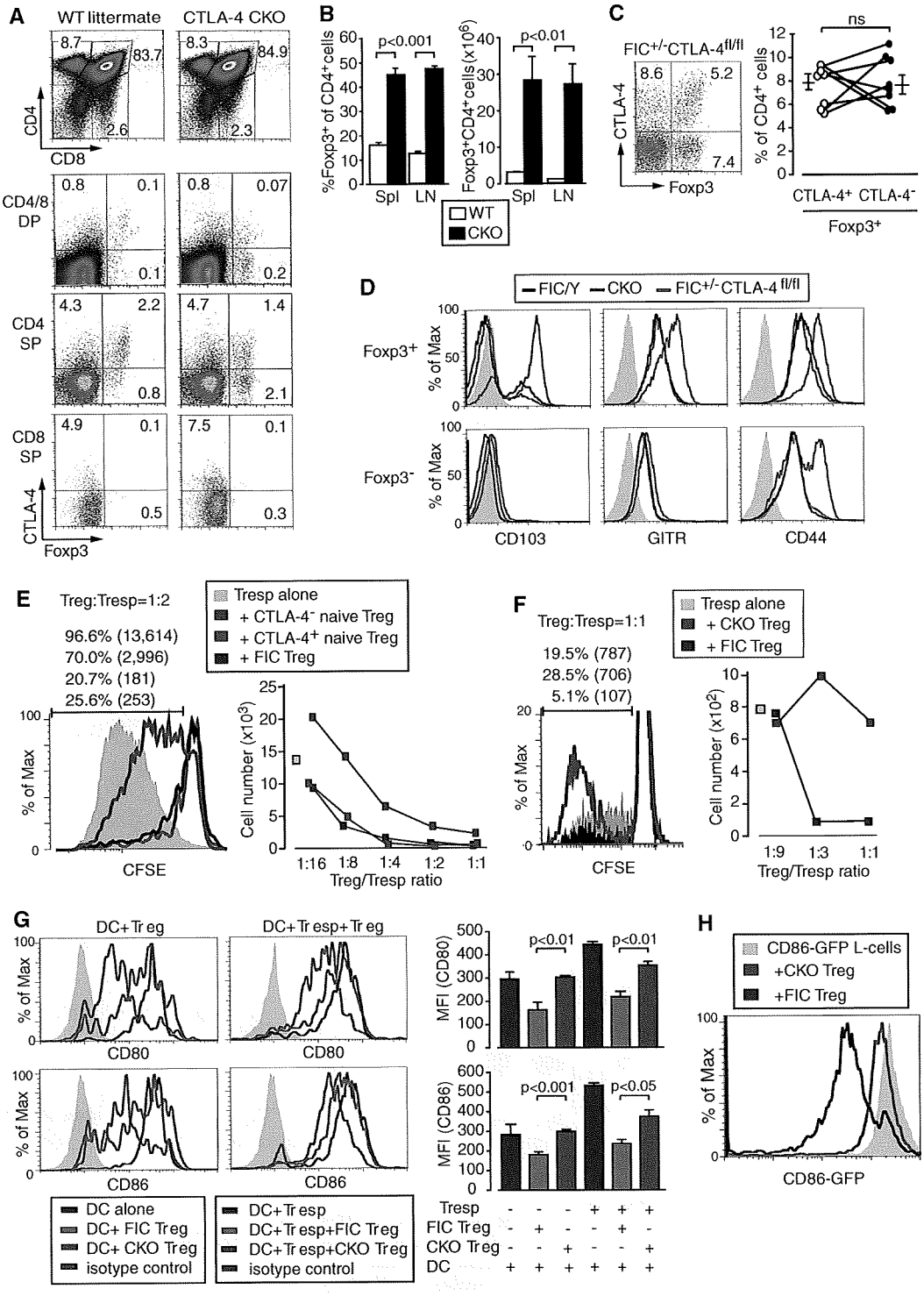

Fig. 4. CTLA-4–deficient Tregs develop and survive normally but have defective function. (**A**) Thymocyte expression of Foxp3 and CTLA-4 in a 2.5-week-old CKO or a WT littermate. SP, single positive; DP, double positive. (**B**) Frequency and number of $CD4^+Foxp3^+$ T cells in spleens and LNs of 6- to 8-week-old CKO or WT littermates (n = 7). (**C**) Foxp3 and CTLA-4 expression in splenic $CD4^+$ T cells from a $FIC^{+/-}$ $CTLA\text{-}4^{fl/fl}$ female mouse (left). Percentages of $Foxp3^+CTLA\text{-}4^+$ and $Foxp3^+CTLA\text{-}4^-$ T cells in each mouse (5 to 8 weeks of age) are connected (n = 8) (right). ns, not significant. (**D**) Expression of cell surface molecules on $CD4^+$ LN cells from CKO, FIC, or $FIC^{+/-}$ $CTLA\text{-}4^{fl/fl}$ mice. (**E**) $CD25^{high}EGFP^+$ cells (naive $CTLA\text{-}4^-$ Treg) and $CD25^{high}EGFP^-$ cells (naive $CTLA\text{-}4^+$ Treg) from $FIC^{+/-}$ $CTLA\text{-}4^{fl/fl}CAG$ female mice and $CD25^{high}CD4^+$ T cells from FIC mice (FIC Treg) were cocultured with $CD25^-CD4^+$ T cells (Tresp), anti-CD3 mAb, and live splenic DCs for 3 days. Percentages and numbers (in parentheses) of CFSE-diluting Tresp cultured at a 1:2 Treg-to-Tresp ratio (left). Numbers of CFSE-diluting Tresp cultured at graded ratios of Treg:Tresp (right). (**F**) Percentage and numbers of CFSE-labeled BALB/c Tresp cocultured with CKO or FIC Tregs and X-irradiated C57BL/6 splenocytes for 4 days at 1:1 Treg:Tresp ratio (left) and numbers at graded ratios (right). (**G**) CD80 and CD86 expression of live splenic DCs after a 2-day culture with Tresp, $CD4^+EGFP^+$ Tregs, or a mix thereof, and anti-CD3 mAb. Histograms show mean fluorescence intensity (MFI). (**H**) L-cells, expressing the Fc receptor, were retrovirally transduced to express CD86-EGFP fusion protein, cocultured with indicated Tregs and anti-CD3 mAb for 2 days, and assessed for GFP level. Data in (A) and (D) to (H) represent three or more independent experiments. Error bars indicate SEM.

CTLA-4–dependent down-regulation of CD80 and CD86 on antigen presenting cells. Tregs probably use multiple suppressive mechanisms, and the importance of each one may vary depending on the environment and the context of immune responses (*1*). However, if the CTLA-4–mediated mechanism of suppression is defective, Tregs cannot sustain self-tolerance and immune homeostasis, even if other suppressive mechanisms become more active to compensate for the deficiency. Thus, CTLA-4 is a key molecular target for controlling Treg-suppressive function in both physiological and pathological immune responses including autoimmunity, allergy, and tumor immunity.

References and Notes

1. S. Sakaguchi *et al.*, *Cell* **133**, 775 (2008).
2. B. Salomon *et al.*, *Immunity* **12**, 431 (2000).
3. T. Takahashi *et al.*, *J. Exp. Med.* **192**, 303 (2000).
4. S. Read, V. Malmstrom, F. Powrie, *J. Exp. Med.* **192**, 295 (2000).
5. S. Hori, T. Nomura, S. Sakaguchi, *Science* **299**, 1057 (2003), published online 9 January 2003; 10.1126/science.1079490.

6. Y. Wu *et al.*, *Cell* **126**, 375 (2006).
7. A. Marson *et al.*, *Nature* **445**, 931 (2007).
8. Y. Zheng *et al.*, *Nature* **445**, 936 (2007).
9. M. Ono *et al.*, *Nature* **446**, 685 (2007).
10. P. Waterhouse *et al.*, *Science* **270**, 985 (1995).
11. E. A. Tivol *et al.*, *Immunity* **3**, 541 (1995).
12. The Wellcome Trust Case Control Consortium, *Nature* **447**, 661 (2007).
13. D. R. Leach, M. F. Krummel, J. P. Allison, *Science* **271**, 1734 (1996).
14. G. Q. Phan *et al.*, *Proc. Natl. Acad. Sci. U.S.A.* **100**, 8372 (2003).
15. S. Read *et al.*, *J. Immunol.* **177**, 4376 (2006).
16. D. M. Sansom, L. S. Walker, *Immunol. Rev.* **212**, 131 (2006).
17. Materials and methods are available as supporting material on *Science* Online.
18. S. Kawamoto *et al.*, *FEBS Lett.* **470**, 263 (2000).
19. M. Ono, J. Shimizu, Y. Miyachi, S. Sakaguchi, *J. Immunol.* **176**, 4748 (2006).
20. Y. Y. Wan, R. A. Flavell, *Nature* **445**, 766 (2007).
21. J. Shimizu, S. Yamazaki, S. Sakaguchi, *J. Immunol.* **163**, 5211 (1999).
22. L. Cederbom, H. Hall, F. Ivars, *Eur. J. Immunol.* **30**, 1538 (2000).
23. C. Oderup, L. Cederbom, A. Makowska, C. M. Cilio, F. Ivars, *Immunology* **118**, 240 (2006).
24. S. Yamazaki, K. Inaba, K. V. Tarbell, R. M. Steinman, *Immunol. Rev.* **212**, 314 (2006).
25. R. J. DiPaolo *et al.*, *J. Immunol.* **179**, 4685 (2007).
26. Y. Onishi *et al.*, *Proc. Natl. Acad. Sci. U.S.A.* **105**, 10113 (2008).
27. We thank M. Ono for discussion and R. Ishii and M. Matsushita for technical assistance. This work was supported by Grants-in-Aid from the Ministry of Education, Sports and Culture of Japan, Japan Science and Technology Agency. Z.F. was a Japan Society for the Promotion of Science fellow, and K.W. was granted a fellowship by Astra-Zeneca, Loughborough, UK.

Supporting Online Material
www.sciencemag.org/cgi/content/full/322/5899/271/DC1
Materials and Methods
SOM Text
Figs. S1 to S13
References

5 May 2008; accepted 15 August 2008
10.1126/science.1160062

Environmental Genomics Reveals a Single-Species Ecosystem Deep Within Earth

Dylan Chivian,[1,2]* Eoin L. Brodie,[2,3] Eric J. Alm,[2,4] David E. Culley,[5] Paramvir S. Dehal,[1,2] Todd Z. DeSantis,[2,3] Thomas M. Gihring,[6] Alla Lapidus,[7] Li-Hung Lin,[8] Stephen R. Lowry,[7] Duane P. Moser,[9] Paul M. Richardson,[7] Gordon Southam,[10] Greg Wanger,[10] Lisa M. Pratt,[11,12] Gary L. Andersen,[2,3] Terry C. Hazen,[2,3,12] Fred J. Brockman,[13] Adam P. Arkin,[1,2,14] Tullis C. Onstott[12,15]

DNA from low-biodiversity fracture water collected at 2.8-kilometer depth in a South African gold mine was sequenced and assembled into a single, complete genome. This bacterium, *Candidatus Desulforudis audaxviator*, composes >99.9% of the microorganisms inhabiting the fluid phase of this particular fracture. Its genome indicates a motile, sporulating, sulfate-reducing, chemoautotrophic thermophile that can fix its own nitrogen and carbon by using machinery shared with archaea. *Candidatus Desulforudis audaxviator* is capable of an independent life-style well suited to long-term isolation from the photosphere deep within Earth's crust and offers an example of a natural ecosystem that appears to have its biological component entirely encoded within a single genome.

A more complete picture of life on, and even in, Earth has recently become possible by extracting and sequencing DNA from an environmental sample, a process called environmental genomics or metagenomics (*1*–*8*). This approach allows us to identify members of microbial communities and to characterize the abilities of the dominant members even when isolation of those organisms has proven intractable. However, with a few exceptions (*5*, *7*), assembling complete or even near-complete genomes for a substantial portion of the member species is usually hampered by the complexity of natural microbial communities.

In addition to elevated temperatures and a lack of O_2, conditions within Earth's crust at depths >1 km are fundamentally different from those of the surface and deep ocean environments. Severe nutrient limitation is believed to result in cell doubling times ranging from 100s to 1000s of years (*9*–*11*), and as a result subsurface microorganisms might be expected to reduce their reproductive burden and exhibit the streamlined genomes of specialists or spend most of their time in a state of semi-senescence, waiting for the return of favorable conditions. Such microorganisms are of particular interest because they permit insight into a mode of life independent of the photosphere.

One bacterium belonging to the *Firmicutes* phylum (Fig. 1A), which we herein name *Candidatus Desulforudis audaxviator*, is prominent in small subunit (SSU or 16*S*) ribosomal RNA (rRNA) gene clone libraries (*11*–*14*) from almost all fracture fluids sampled to date from depths greater than 1.5 km across the Witwatersrand basin (covering 150 km by 300 km near Johannesburg, South Africa). This bacterium was shown in a previous geochemical and 16*S* rRNA gene study (*11*) to dominate the indigenous microorganisms found in a fracture zone at 2.8 km below land surface at level 104 of the Mponeng mine (MP104). Although Lin *et al.* (*11*) discovered that this fracture zone contained the least-diverse natural free-living microbial community reported at that time, exceeding the ~80% dominance by the methanogenic archaeon IUA5/6 of a comparatively shallow subsurface community in Idaho (*15*), we were nonetheless surprised when the current environmental genomics study revealed only one species was actually present within the fracture fluid. Furthermore, we found that the genome of this organism appeared to possess all of the metabolic capabilities necessary for an independent life-style. This gene complement was consistent with the previous geochemical and thermodynamic analyses at the ambient ~60°C temperature and pH of 9.3, which indicated radiolytically generated chemical species as providing the energy and nutrients to the system (*11*), with formate and H_2 as possessing the greatest potential among candidate electron donors, and sulfate (SO_4^{2-}) reduction as the dominant electron-accepting process (*11*).

DNA was extracted from ~5600 liters of filtered fracture water by using a protocol that has been demonstrated to be effective on a broad range of bacterial and archaeal species, including recalcitrant organisms (*16*). A single, complete, 2.35–megabase pair (Mbp) genome was assembled with a combination of shotgun Sanger sequencing and 454 pyrosequencing (*16*). Similar to other studies that obtained near-complete consensus genomes from environmental samples (*5*, *17*), heterogeneity in the population of the dominant species as measured with single-nucleotide polymorphisms (SNP) was quite low, showing only 32 positions with a SNP observed

[1]Physical Biosciences Division, Lawrence Berkeley National Laboratory, Berkeley, CA 94720, USA. [2]Virtual Institute for Microbial Stress and Survival, Berkeley, CA 94720, USA. [3]Earth Sciences Division, Lawrence Berkeley National Laboratory, Berkeley, CA 94720, USA. [4]Departments of Biological and Civil and Environmental Engineering, Massachusetts Institute of Technology, Cambridge, MA 02139, USA. [5]Energy and Efficiency Technology Division, Pacific Northwest National Laboratory, Richland, WA 99352, USA. [6]Department of Oceanography, Florida State University, Tallahassee, FL 32306, USA. [7]Genomic Technology Program, U.S. Department of Energy (DOE) Joint Genomics Institute, Berkeley, CA 94598, USA. [8]Department of Geosciences, National Taiwan University, Taipei 106, Taiwan. [9]Division of Earth and Ecosystem Sciences, Desert Research Institute, Las Vegas, NV 89119, USA. [10]Department of Earth Sciences, University of Western Ontario, London, ON N6A 5B7, Canada [11]Department of Geological Sciences, Indiana University, Bloomington, IN 47405, USA. [12]Indiana Princeton Tennessee Astrobiology Initiative (IPTAI), NASA Astrobiology Institute, Bloomington, IN 47405, USA. [13]Biological Sciences Division, Pacific Northwest National Laboratory, Richland, WA 99352, USA. [14]Department of Bioengineering, University of California, Berkeley, CA 94720, USA. [15]Department of Geosciences, Princeton University, Princeton, NJ 08544, USA.

*To whom correspondence should be addressed. E-mail: DCChivian@lbl.gov

International Immunology, Vol. 20, No. 10, pp. 1331–1342
doi:10.1093/intimm/dxn091

FEATURED ARTICLE

Arthritis and pneumonitis produced by the same T cell clones from mice with spontaneous autoimmune arthritis

Chiaki Wakasa-Morimoto[1], Tomoko Toyosaki-Maeda[1], Takaji Matsutani[2], Ryu Yoshida[1], Shino Nakamura-Kikuoka[1], Miki Maeda-Tanimura[1], Hiroyuki Yoshitomi[3], Keiji Hirota[3], Motomu Hashimoto[3], Hideyuki Masaki[4], Yoshiki Fujii[5], Tsuneaki Sakata[1], Yuji Tsuruta[1], Ryuji Suzuki[6], Noriko Sakaguchi[3] and **Shimon Sakaguchi[3]**

[1]Discovery Research Laboratories, Shionogi & Co., Ltd, 2-5-1 Mishima Settsu-shi, Osaka 566-0022, Japan
[2]Department of Cell Biology, Tohoku University School of Medicine, 2-1 Seiryo-machi, Sendai 980-8575, Japan
[3]Department of Experimental Pathology, Institute for Frontier Medical Sciences, Kyoto University, 53 Shogoin Kawahara-cho, Sakyo-ku, Kyoto 606-8507, Japan
[4]Department of Biochemistry, Kinki University School of Medicine, 377-2 Ohno-higashi, Osakasayama-shi, Osaka 589-8511, Japan
[5]Department of Virology 1, National Institute of Infectious Diseases, 1-23-1 Toyama, Shinjuku-ku, Tokyo 162-8640, Japan
[6]Clinical Research Center for Rheumatology and Allergy National Sagamihara Hospital, 18-1 Sakuradai, Sagamihara-shi, Kanagawa 228-8522, Japan

Keywords: animal model, interstitial lung disease, rheumatoid arthritis, T cell clone

Abstract

SKG mice, a newly established model of rheumatoid arthritis (RA), spontaneously develop autoimmune arthritis accompanying extra-articular manifestations, such as interstitial pneumonitis. To examine possible roles of T cells for mediating this systemic autoimmunity, we generated T cell clones from arthritic joints of SKG mice. Two distinct $CD8^+$ clones were established and both showed *in vitro* autoreactivity by killing syngeneic synovial cells and a variety of MHC-matched cell lines. Transfer of each clone to histocompatible athymic nude mice elicited joint swelling and histologically evident synovitis accompanying the destruction of adjacent cartilage and bone. Notably, the transfer also produced diffuse severe interstitial pneumonitis. Clone-specific TCR gene messages in the inflamed joints and lungs of the recipients gradually diminished, becoming hardly detectable in 6–11 months; yet, arthritis and pneumonitis continued to progress. Thus, the same $CD8^+$ T cell clones from arthritic lesions of SKG mice can elicit both synovitis and pneumonitis, which chronically progress and apparently become less T cell dependent in a later phase. The results provide clues to our understanding of how self-reactive T cells cause both articular and extra-articular lesions in RA as a systemic autoimmune disease.

Introduction

Rheumatoid arthritis (RA) is a chronic inflammatory disease of unknown etiology that primarily affects the synovial membranes of multiple joints (1, 2). A cardinal feature of joint inflammation in RA is proliferative inflammation of the synovium, i.e. synovitis, which leads to the destruction of adjacent cartilage and bone. In addition, RA frequently accompanies extra-articular manifestations, for example the development of rheumatoid factors, rheumatic nodules, vasculitis and interstitial lung disease (ILD). Recent studies with high-resolution imaging have indeed revealed a high prevalence of ILD in patients with RA (3–6). RA is thus a systemic disease; yet, the immunological basis of this systemic autoimmunity is poorly understood.

T cells appear to play a key role in the development of RA as suggested by the infiltration of T cells, especially $CD4^+$ T cells, into the synovial tissue of RA (7–9) and the association of genetic susceptibility to RA with particular alleles of HLA-DR (10, 11). On the other hand, there is evidence in humans and animal models that stimulated synoviocytes, composed of macrophage-like and fibroblast-like synovial cells, can

Correspondence to: S. Sakaguchi; E-mail: shimon@frontier.kyoto-u.ac.jp

Transmitting editor: K. Yamamoto

Received 31 March 2008, *accepted* 17 July 2008

Advance Access publication 18 August 2008

themselves mediate joint destruction in a T cell-independent manner (12, 13). A key issue in elucidating the pathogenetic mechanism of RA is, therefore, to determine how self-reactive T cells contribute to the initiation and progression of synovitis and possibly extra-articular lesions such as ILD.

The SKG strain of mice spontaneously develops T cell-mediated chronic autoimmune arthritis (14–16). The strain possesses a mutation in the gene encoding a Src homology 2 domain of the ζ-associated protein of 70 kDa (ZAP-70), a key signal transduction molecule in T cells (17, 18). Impaired signal transduction through SKG ZAP-70 results in thymic positive selection and failure in negative selection of highly self-reactive T cells that include potentially arthritogenic T cells (14). The SKG arthritis progresses chronically, starting from small joints of the digits and symmetrically progressing to larger joints, such as the wrists and ankles. Histologically, affected joints show hyperplasia of synoviocytes, inflammatory cell infiltration, pannus formation and destruction of cartilage and bone, eventually leading to joint deformity. As extra-articular lesions, they develop interstitial pneumonitis, dermatitis, necrobiotic nodules akin to rheumatic nodules in RA and systemic vasculitides. Serologically, they spontaneously develop IgM-type rheumatoid factors, auto-antibodies against type II collagen and antibodies cross-reactive with *Mycobacterium tuberculosis* heat shock protein (hsp) 70. IL-1, tumor necrosis factor (TNF)-α, IL-6 or IL-17 deficiency inhibits the development of arthritis in SKG mice (15, 19), similar to the effects of anti-cytokine therapies in RA (20, 21). Thus, autoimmune disease in SKG mice closely resembles RA in clinical and immunopathological characteristics. In addition, considering recent findings that genetic polymorphism of a signaling molecule at a TCR proximal step involving ZAP-70 significantly contributes to the susceptibility to RA and other autoimmune diseases (22, 23), SKG mice can be a suitable model for elucidating how a T cell-intrinsic anomaly contributes to the development of RA as a systemic autoimmune disease.

In this study, we have attempted to determine the role of T cells in SKG autoimmune disease by establishing T cell clones from their arthritic lesions. We have established two distinct $CD8^+$ clones and show that both of them have the potential to induce not only arthritis but also pneumonitis. This indicates that inflammation in both the joints and the lung can be mediated, at least in part, by common autoreactive T cell clones in SKG mice. In addition, by adoptively transferring these T cell clones to normal mice, we show that autoreactive T cells are able to initiate arthritis; yet, the arthritis can progress apparently in a T cell-independent manner in a later phase. These findings contribute to our understanding of how T cells cause chronic arthritis and ILD in RA.

Materials and methods

Mice

SKG and (SKG × BALB/c)F_1 mice (14) were maintained in the animal facility of Kyoto University under a microbially conventional condition. Female C.B-17 SCID mice (Clea Japan, Tokyo, Japan), DBA/1J, BALB/c and BALB/c-nu/nu mice (Charles River Japan, Kanagawa, Japan) were maintained under specific pathogen-free conditions at Kyoto University or Discovery Research Laboratories of Shionogi & Co., Ltd. All experiments were approved by the Animal Care and Use Committee at Kyoto University and Shionogi & Co., Ltd.

Culture medium

The culture medium for SKG T cell lines and clones was AIM-V supplemented with 20% RPMI-1640, 1 mM sodium pyruvate, 50 μM 2-mercaptoethanol (ME), 2 mM L-glutamine, ×1 penicillin/streptomysin (Gibco BRL, Gaithersburg, MD, USA), 10% heat-inactivated FCS (Hyclone, Logan, UT, USA), 10% rat T-STIM™ with Con A (Becton Dickinson, Franklin Lakes, NJ, USA), 100 U/ml of recombinant mouse IL-2 (Genzyme, Cambridge, MA) and 5 μg/ml of Con A (Sigma, St Louis, MO, USA).

Establishment of T cell clones from arthritic joints of SKG mice

To establish T cell lines, severely swollen joints of SKG mice were aseptically excised, finely minced and cultured until clusters of mononuclear cells were confirmed in bulk culture. Outgrown T cells were cloned in 96-well microplates by using SKG synovial cells (1×10^3) as feeder cells. Synovial cells were prepared as previously described (16). Briefly, synovial tissues from wrist and ankle joints were digested with 400 Mandl U/ml of Liberase Brendzyme II (Roche) in RPMI-1640 medium for 1 h at 37°C; digested cells were filtrated through a nylon mesh to prepare single-cell suspensions. A typical composition of the synoviocyte preparation was ~10% $CD11b^+$ monocyte/macrophages, ~20% $Gr\text{-}1^+$ granulocytes, ~1% T cells and other cells. Several days later non-adherent cells were removed by washing the plates with culture medium. T cells that had outgrown from the bulk culture of synovial cells were dispensed at 1, 5, 20 or 50 cells per well and apparently single colonies were propagated in the culture medium described above. Clonality of each cell was confirmed by microplate hybridization assay (MHA) (24) and sequence analysis of TCR. Established T cell clones were maintained without feeder cells. Dengue 2F7 and 3F2 T cell clones, established by immunization of BALB/c mice with the NS3 peptide of dengue virus, were kindly provided by Dr H. Masaki (Kinki University). All cultures were performed in a humidified atmosphere of 7.5% CO_2 at 37°C.

Cytokine detection

Cytokine production by T cell clones were analyzed by ELISA. T cell clones were stimulated with 10 ng/ml of phorbol myristate acetate (PMA) (Wako Chemicals USA, Inc., Richmond, VA, USA) and 0.4 μg/ml of ionomycin (Calbiochem, Darmstadt, Germany) in culture medium at 1×10^6 cells/ml for 16 h. The supernatants were assayed for various cytokines using specific ELISA kits (Endogen, Woburn, MA, USA, and Axis-Shield, Oslo, Norway) according to the manufacturer's protocol. Cytokine mRNA levels in the joints and lungs of clone recipient mice were analyzed by quantitative PCR as described previously (25).

MHA for TCR AV and BV family and sequence analysis

MHA, cDNA synthesis and PCR amplifications of TCR of each T cell clone were performed as described previously (24). The

PCR products cloned into a pGEM-T Easy vector (Promega, Madison, WI, USA) were analyzed for TCR sequences using CEQ DTCS-Quick Start Kit according to the manufacturer's protocol (Beckman Coulter Inc., Fullerton, CA, USA).

^{51}Cr release cytotoxicity assay

BALB/3T3 fibroblast line (H-2^d), J774 macrophage line (H-2^d), p815 mastocytoma line (H-2^d), EL-4 lymphoma line (H-2^b), L929 fibroblast line (H-2^k) obtained from Dainippon Sumitomo Pharma (Osaka, Japan) and synovial cells of SKG mice (H-2^d) were used as target cells. Synovial cells (1×10^4) were seeded in 96-well flat-bottom plates with 40 U/well of IFN-γ for 2 days and radiolabeled with 2.5 μCi/well of $Na_2^{51}CrO_4$ (Daiichi Radioisotope Laboratories, Ltd, Tokyo, Japan) for 2 h. Other target cells (3×10^5) were radiolabeled with 20 μCi of $Na_2^{51}CrO_4$ for 2 h and seeded in 96-well round-bottom plates at 1×10^4 cells per well. Effector cells (4×10^5) were added in each well in triplicate and incubated for 8 h. Relative cytotoxicity was calculated as follows from the radioactivity released in the culture supernatant; percent specific lysis = 100(experimental − spontaneous)/(maximal − spontaneous) counts per minute. Maximal lysis and spontaneous release were determined from target cells incubated with surfactant ×7 (Flow Laboratories, ICN Biomedicals, Inc., Aurora, OH, USA) or without effector cells, respectively.

Adoptive transfer

Spleen T cells from SKG mice or (SKG × BALB/c)F_1 mice and each SKG T cell clones (1×10^7) were intravenously transferred to C.B-17 SCID mice (8 weeks) or BALB/c-nu/nu mice (6 weeks), respectively. Control dengue 2F7 and 3F2 clone were collected 10–14 days after *in vitro* stimulation with specific peptide-pulsed irradiated (33 Gray) BALB/c spleen cells and transferred as described above. Severity of arthritis was scored weekly as previously described (14).

Clinical assessment of arthritis

Joint swelling was monitored by inspection and scored as follows: 0, no joint swelling; 0.1, swelling of one finger joint; 0.5, mild swelling of wrist or ankle and 1.0, severe swelling of wrist or ankle. Scores for all fingers and toes, wrists and ankles were totalled for each mouse (14).

Histological assessment of interstitial pneumonitis

Interstitial pneumonitis was evaluated microscopically depending on diffusely affected area: –, normal histology; +, 10–30%; ++, 30–60%; +++, >60% of the sections of the lungs showed pneumonitis.

Histology and immunohistochemistry

Tissues were fixed in 10% neutral formalin, paraffin embedded and stained with Haematoxylin & Eosin (H&E). Joints were additionally decalcified for 3 weeks in 10% EDTA in PBS before staining. For immunohistochemistry of joints, deparaffinized sections were incubated with 20% normal rabbit serum (Dako, Hamburg, Germany) in PBS for 15 min to block non-specific binding, primary rat anti-Ly-6G mAb (Gr-1, RB6-8C5; BD PharMingen) with appropriate dilutions overnight at 4°C, biotinylated polyclonal rabbit anti-rat antibody (Dako) and HRP-conjugated streptavidin (Dako). The slides were developed using diaminobenzidene (Elite Kit; Vector, Burlingame, CA, USA) and counterstained with Mayer's hematoxylin.

For immunohistochemistry of lungs, tissues were fixed in 4% phosphate-buffered PFA (pH 7.4) and embedded in Tissue-Tek OCT compound (Ted Pella, Inc., Redding, CA, USA). Cryostat sections were stained with rat mAbs to mouse CD4 (H129.19), CD8a (53-6.7), CD45R/B220 (RA3-6B2), Ly-6G (RB6-8C5) (BD PharMingen) and F4/80 (Cl: A3-1) (CALTAG Laboratories, Burlingame, CA, USA) with appropriate dilutions followed by incubation with biotinylated secondary antibodies and HRP-conjugated streptavidin. The slides were developed as described above.

Southern blot analysis

The persistence of transferred clones in the recipients was assessed by Southern blot analysis. Two micrograms of total RNA of each tissue was treated with DNaseI and reverse transcribed using Superscript II (Invitrogen, Carlsbad, CA, USA). Nested PCRs were performed as described previously (24) to amplify TCR β chain of 35S or dengue 2F7 with the primers specific for V, J and C region. Ten microliters of the PCR products were separated on 2% agarose gel, transferred onto Hybond-N+ membranes (Amersham Biosciences, Piscataway, NJ, USA) according to the manufacturer's instructions. The membranes were prehybridized overnight with PerfectHyb (TOYOBO CO., Ltd, Osaka, Japan) at 54°C and hybridized with the third complementarity-determining region (CDR3)-specific probes labeled with ^{32}P-deoxyadenosine triphosphate for 3 h at 54°C. The membranes were washed in ×2 standard saline citrate (SSC) and 0.1% SDS at room temperature and ×0.2 SSC and 0.1% SDS at 37°C. RNA extracts of 35S and dengue 2F7 clones, diluted to 1% of concentration with RNA of L9 cells, were used as positive controls. The detection limits of 35S and dengue 2F7 were compared using the serial dilution of positive controls and both systems detected the RNA extract corresponding to the amount of one cell.

The sequences of PCR primers and probes are as follows; 35S: first PCR (BV8S3-1: 5′-ATA TGG TGC TGG CAA CCT TC-3′ and MCB1: 5′-AGG ATT GTG CCA GAA GGT AG-3′), second PCR (BV8S3-2: 5′-ACC AGA ACA ACG CAA GAA GAC T-3′ and MCB2: 5′-TTG TAG GCC TGA GGG TCC-3′), third PCR (BV8S3-3: 5′-TTC CTC CTG CTG GAA TTG GC-3′ and BJ1.5: 5′-TAG AAC AGA GAT CGA GTC CC-3′) and probe (5′-AGT GGG ACA GGG GGC AAC CA-3′). Dengue 2F7: first PCR (BV8S1-1: 5′-CCC AAA GTC CAA GAA GCA AG-3′ and MCB1), second PCR (BV8S1-2: 5′-GTA CAA GGC CTC CAG ACC AA-3′ and MCB2), third PCR (BV8S1-3: 5′-TGG CTT CCC TTT CTC AGA CA-3′ and BJ2.7: 5′-AAG GAG ACC TTG GGT GGA GT-3′) and probe (5′-TGC CAC CAA CGA CAA CTC CT-3′).

Results

Induction of arthritis and interstitial pneumonitis in SCID mice by the transfer of SKG splenic T cells

In our conventional housing environment, SKG mice started to develop arthritis around 2 months of age and

histologically evident mild interstitial pneumonitis around 6 months of age (14). To determine the role of T cells in SKG mouse autoimmunity, we transferred splenic T cells from 3-month-old arthritic SKG mice (without histologically evident pneumonitis or colitis) to T/B-cell-deficient C.B-17 SCID mice, which are histocompatible with SKG mice on the BALB/c background (14). Within 2 months after transfer, the recipient developed arthritis (14) and mild but histologically evident interstitial pneumonitis (Table 1, Fig. 1); they also developed mild colitis (data not shown). Similar cell transfer from non-arthritic heterozygotes of the SKG mutation failed to induce such lesions in the recipients. Age-matched SCID mice similarly maintained in our facility did not develop these lesions histologically (data not shown). The results thus indicate that SKG T cells are able to adoptively transfer arthritis and also have a potential to induce interstitial pneumonitis and colitis when transferred to SCID mice.

Establishment of T cell clones from arthritic joints

To analyze the mechanism of such T cell-mediated inflammatory tissue damage in multiple organs, we attempted to establish T cell clones from arthritic joints of SKG mice, as described in Materials and methods. Two T cell clones, designated 35S and 73S, were established in separate experiments. The clones were maintained and expanded with culture medium containing IL-2 and Con A (see Materials and methods). $CD8^+$ CTL clones specific for dengue virus NS3 protein were used as control.

Cytofluorometric analyses revealed that the 35S and 73S clones were $CD8^+$. Both expressed α and β chains of the TCR, and the expression level of the TCR on 35S was slightly lower than normal (Fig. 2). In response to *in vitro* PMA and ionomycin stimulation, 35S and 73S produced IFN-γ but no detectable amount of TNF-α, IL-4, IL-5, IL-6, IL-10 or IL-17 by ELISA (Table 2).

Clonality of each T cell line was confirmed by MHA (24) (data not shown) and sequence analysis of the TCR α and β chains with determination of the amino acid sequences of the TCRs (Table 3). Interestingly, these T cell clones shared in common the BV8S3 TCR Vβ subfamily; yet, the CDR3 sequences of the TCR β chains were different (26–29).

Table 1. Induction of arthritis, interstitial pneumonitis and colitis in SCID mice by the transfer of SKG splenic T cells

Spleen cell donor	Recipients	Arthritis	Interstitial pneumonitis	Colitis
SKG	1	++ (4.6)	++	+
	2	++ (4.0)	++	+
	3	++ (4.0)	+	+
	4	++ (3.0)	+	–
(SKG × BALB/c)F_1	1	–	–	–
	2	–	–	–
	3	–	–	–
	4	–	–	–

Cells (1×10^7) of T cells prepared from spleens of indicated mice were intravenously transferred to 8-week-old SCID mice. The severity of arthritis, interstital pneumonitis and colitis in these mice was histologically assessed 2 months later.

Autoreactivity of T cell clones

In ^{51}Cr release cytotoxicity assay to determine cytotoxic activity of the SKG clones against syngeneic synovial cells, 35S and 73S lysed SKG synovial cells prepared by crude collagenase digestion of inflamed synovium (44.0 and 16.3% of specific lysis, respectively, at a high 40:1 ratio), while control dengue 2F7 clone did not (Fig. 3A). 35S lysed not only syngeneic synovial cells but also MHC-matched cell lines, such as BALB/c-derived 3T3 cells, macrophage-like J774 cells and DBA/2 ($H\text{-}2^d$)-derived P815 cells, whereas the clone failed to lyse allogenic EL-4 ($H\text{-}2^b$) lymphoid or L929 ($H\text{-}2^k$) fibroblast cell line (Fig. 3B). Thus, 35S appears to recognize a ubiquitous self-peptide in an MHC-restricted manner. These

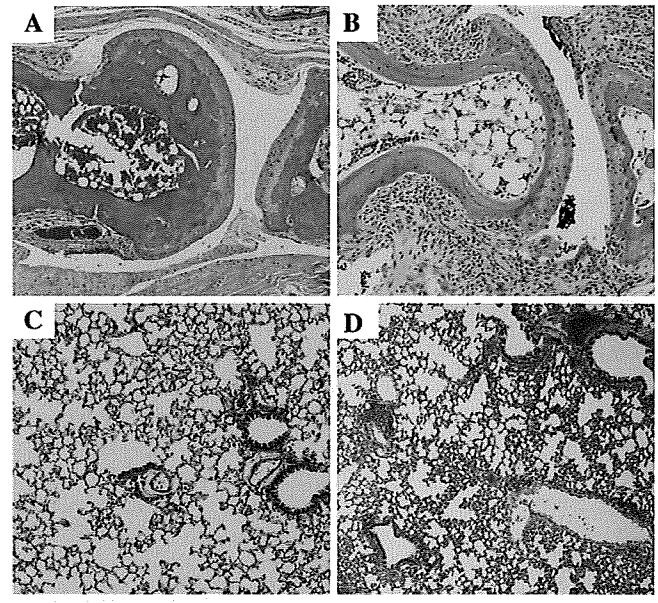

Fig. 1. Arthritis and pneumonitis in SCID mice transferred with T cells from SKG mice. Histology of a joint (A) and lung (C) of a SCID mouse T cell transferred from (SKG × BALB/c)F_1 mouse. Arthritis (B) and interstitial pneumonitis (D) in a SCID mouse T cell transferred from a SKG mouse. H&E staining (A and B, ×100; C and D, ×50).

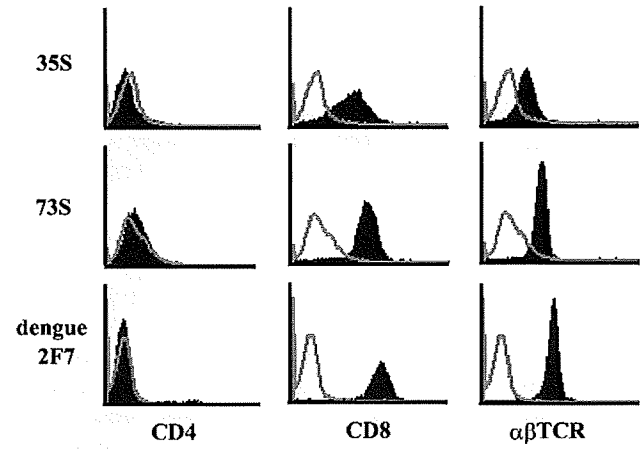

Fig. 2. Expression levels of CD4, CD8 and αβ TCR on 35S, 73S and dengue 2F7 clones.

functional characteristics, together with cell surface and cytokine-secreting profiles, indicate that 35S and 73S are CTL and that they bear self-reactive specificity.

Induction of synovitis in BALB/c nude mice by adoptive transfer of T cell clones

To examine possible arthritogenicity of the T cell clones, they were transferred to BALB/c nude mice once, and the degree of joint swelling of each recipient mouse was assessed once a week for 12 months (Fig. 4). Transfer of 35S and 73S clones induced joint swelling with incidences of 57.1% (4 out of 7 mice) and 42.9% (3 out of 7 mice), respectively, during the observation period; synovitis was histologically evident in 71.4% (5 out of 7 mice) in each transfer (Table 4, Fig. 5). Once joint swelling started in one joint following cell transfer, it slowly progressed with remissions and exacerbations, leading to swelling of other joints in a symmetrical fashion (Figs 4 and 5A–D). Two mice showed progressive debilitation to death without an apparent cause, although one of them showed dermatitis; with debilitation, joint swelling somehow remitted in these mice.

Table 2. Cytokine production (ng/ml) of T cell clones derived from SKG joints and control clones

	TNF-α	IFN-γ	IL-4	IL-5	IL-10	IL-6	IL-17
35S	0.02	180	0.03	<0.02	<0.04	0.2	<0.01
73S	0.02	80	0.03	<0.02	1.2	<0.05	<0.01
Dengue 2F7	0.2	10	ND	ND	<0.04	<0.05	<0.01
Dengue 3F2	0.02	20	ND	ND	<0.04	<0.05	<0.01

Culture supernatant of activated cells by PMA and ionomycin for 16 h were assayed by ELISA. ND, not done.

Table 3. CDR3 sequences of the TCR α and β chain used by the SKG T cell clones

TCR α chains	AV	V	N	J	AJ
35S	3S6	C A V T	S D	S G T Y Q R F	13
73S	3S1	C A A S M	R R	N S G T Y Q R F	13
Dengue 2F7	2S2/7	C A A		N Q G G R A L I F	15
Dengue 3F2	2S2/7	C A A	S G R D	Y A N K M I F	47
TCR β chains	**BV**	**V**	**N-D-N**	**J**	**BJ**
35S	8S3	C A S S G	T G G	N Q A P L F	1.5
73S	8S3	C A S S G	W G D	A E Q F F	2.1
Dengue 2F7	8S1	C A T	N D N	S Y E Q Y E	2.7
Dengue 3F2	8S2	C A S E	T R	E Q Y F	2.6

The amino acid sequences of the V, D and J regions of the TCR were determined according to the nucleotide sequences. AV and BV gene families were assigned according to Arden *et al.* (26). AJ genes were numbered according to Koop *et al.* (27). BJ genes were assigned according to Malissen *et al.* (28) and Gascoigne *et al.* (29).

Histologically, swollen joints showed marked synovial and peri-articular inflammation when examined 6–12 months after cell transfer (Fig. 5E and F). The inflammation accompanied a marked proliferation of synovial lining cells, infiltration of inflammatory cells into subsynovial tissue and joint cavity and active angiogenesis; pannus eroded the adjacent cartilage and bone (Fig. 5F). Gr-1-positive neutrophils were abundant among the infiltrating cells, as observed in the arthritic lesions of SKG mice (14, 15), whereas few T cells infiltrated into the inflammation sites (Fig. 5G and H).

In accordance with the appearance of multinuclear cells at the interface between proliferating synoviocytes and bone, many tartrate-resistant acid phosphatase-positive osteoclasts were observed in the inflamed joints (Fig. 6A–D). Safranin-O staining revealed a decrease in proteoglycan in the articular cartilage matrix of severely affected joints (Fig. 6E and F). Notably, Gr-1-positive cells, mainly neutrophils, also increased in the bone marrow (BM) of the affected recipients (Fig. 6G and H).

A high level of circulating rheumatoid factors was detected in one mouse out of seven recipients of the 35S clone and in none of the recipients of other clones (data not shown).

Some of the swollen joints following transfer of 35S $CD8^+$ clones exhibited higher expression levels of IL-17 mRNA assessed by quantitative reverse transcription (RT)–PCR than those from mice transferred with control $CD8^+$ clones (Supplementary Figure 1A, available at *International Immunology* Online), despite that 35S failed to produce IL-17 upon *in vitro* stimulation.

Taken together, the $CD8^+$ T cell clones prepared from arthritic lesions of SKG mice were able to induce arthritis in athymic nude recipients, leading to the destruction of the surrounding cartilage and the bone.

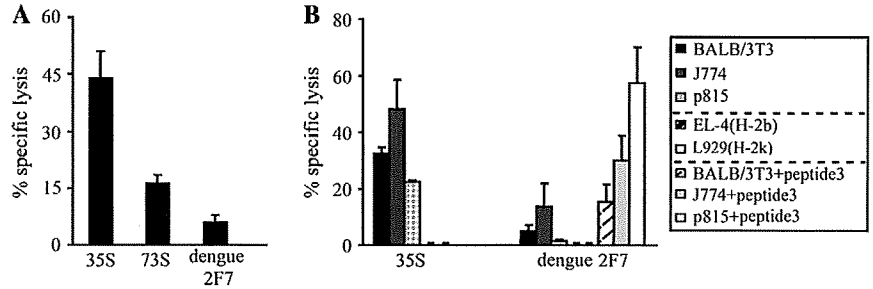

Fig. 3. *In vitro* self-reactivity of SKG T cell clones. (A) CTL activity of SKG T cell clones against SKG synovial cells. CTL clones specific for dengue virus NS3 protein, dengue 2F7, was used as control. IFN-γ-treated target cells were ^{51}Cr labeled in adherent condition and incubated with effector cells for 8 h (E:T ratio = 40). (B) CTL activity of SKG T cell clones against various types of cell lines (E:T ratio = 40). CTL activity of dengue 2F7 clone was also analyzed against H-2^d cells pulsed with a specific peptide (E:T ratio = 10). All assays were conducted in triplicate with 8 h of incubation. The mean and standard deviation of three independent experiments are shown in each bar.

Induction of interstitial pneumonitis in BALB/c nude mice by the transfer of T cell clones

Notably, histologically evident severe alveolitis and diffuse interstitial pneumonitis also developed in all the recipients of 35S and 73S but not in those recipients of dengue 2F7 and 3F2 clones (Table 4 and Fig. 7A–D). Some recipients of 35S and 73S developed only pneumonitis without histologically evident synovitis. No histologically apparent inflammation was observed in other tissues/organs including the liver and the colon in any of these recipient mice (data not shown). The diffuse pulmonary lesions (Fig. 7A and B) comprised thickening of the alveolar walls, and perivascular and peribronchiolar infiltration by inflammatory cells (Fig. 7C and D). Immunohistochemical analysis of the 73S recipients 6 months after cell transfer revealed the infiltration of a large number of granulocytes as Gr-1$^+$ cells (Fig. 7E), macrophages as F4/80$^+$ cells (Fig. 7F) and B cells as B220$^+$ cells (Fig. 7G) into the alveolar walls and spaces and also the perivascular and peribronchiolar area where only a small number of CD8$^+$ T cells were detected, which might be transferred to CD8$^+$ clones or derived from nude mice (30) (Fig. 7H). CD4$^+$ T cells were occasionally found in the lesions and could be those derived from endogenous T cells that might develop extrathymically in aged nude mice (Fig. 7I) (30).

The pulmonary tissues with severe interstitial pneumonitis following CD8$^+$ clone transfer exhibited higher expression levels of IL-17 mRNA by quantitative RT–PCR compared with the mice transferred with control CD8$^+$ clones (Supplementary Figure 1B, available at *International Immunology* Online).

Thus, the SKG arthritogenic T cell clones are able to induce interstitial pneumonitis when transferred to athymic nude mice.

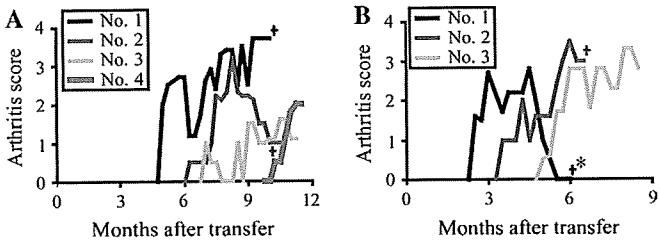

Fig. 4. Time course of joint swelling in the recipient mice of SKG T cell clones, 35S (A) and 73S (B). Score for all paws were totalized for each mouse. +, Sacrificed at the indicated time points; *, the mouse developed dermatitis at 5 months after transfer.

Detection of transferred clones in recipient mice

Since T cells were hardly detected by immunohistochemistry at the site of synovitis or pneumonitis 6 months after clone transfer (data not shown and see above), the persistence of transferred clones in the recipients was assessed by RT–PCR amplification of TCR β chain gene and Southern blot analysis of the products with a CDR3 sequence-specific probe. We adopted this method to avoid detecting nude mouse-derived oligoclonal endogenous T cells that may expand with aging (see above) (30–32). For example, a clone-specific TCR message of the 35S clone was detected in the majority of recipient spleens 1 month after transfer but not in the spleens examined 6 months later (Fig. 8). As shown in Fig. 9, the messages were

Table 4. Development of arthritis and interstitial pneumonitis in BALB/c nude mice transferred with T cell clones

Clone	Individual recipients	Macroscopically evident arthritis			Histological analysis	
		Onset (months)	Sacrifice (months)	Clinical score[a]	Synovitis[b]	Interstitial pneumonitis[c]
35S	1	5	10	3.7	++	+
	2	6	11	3.2	++	++
	3	7	11	1.6	++	+++
	4	10	12	2.0	++	+++
	5	–	9	0	+	±
	6	–	12	0	—	+++
	7	–	12	0	—	+++
73S	1	2.5	6	2.8	++	++
	2	3.5	6	3.5	++	+
	3	5	9	3.3	++	++
	4	–	8	0	+	++
	5	–	9	0	+	+++
	6	–	12	0	—	++
	7	–	12	0	—	++
Dengue 2F7	1	–	9	0	—	—
	2	–	9	0	—	—
	3	–	9	0	—	—
	4	–	9	0	—	—
	5	–	12	0	—	—
	6	–	12	0	—	—
	7	–	12	0	—	—
Dengue 3F2	1	–	12	0	—	—
	2	–	12	0	—	—

Six-week-old BALB/c nude mice were intravenously injected with 1×10^7 cells of each clone. The incidence of joint swelling of the recipient mice was examined weekly. Mice were sacrificed 6–12 months after cell transfer.

[a]Maximum clinical score of arthritis.

[b]–, Without change; +, microscopically observed synovitis without joint swelling; ++, macroscopically obvious joint swelling.

[c]–, Normal histology; +, 10–30%; ++, 30–60%; +++, >60% of the sections of the lungs showed pneumonitis (Fig. 7).

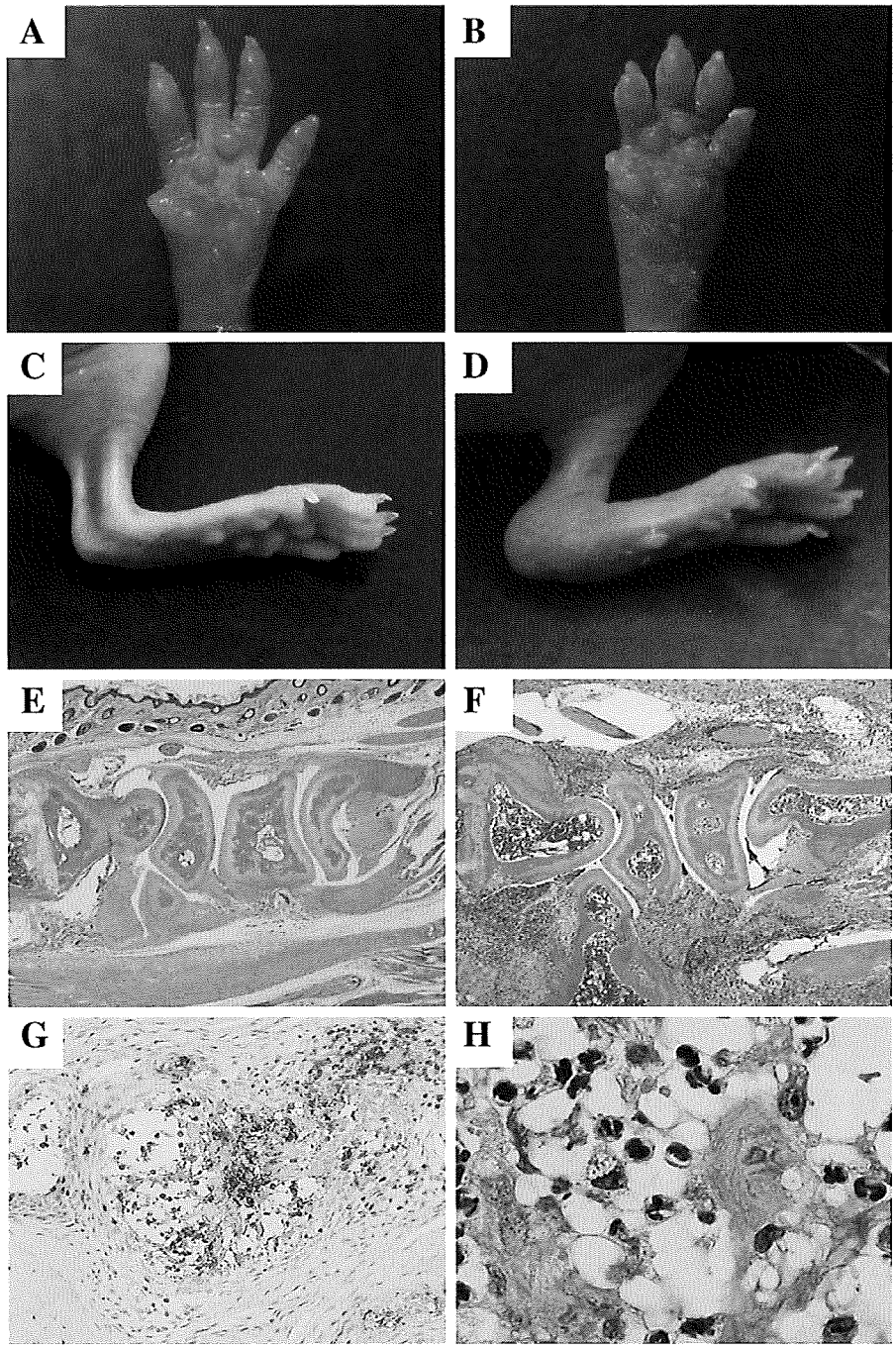

Fig. 5. Arthritis in athymic nude mice transferred with SKG T cell clones. (A–D) Macroscopic views of a forepaw (A) and a hind paw (C) of a recipient of control dengue 2F7 and a forepaw (B) and a hindpaw (D) of a recipient of 35S. (E–H) Histology of the joints of recipients of control dengue 2F7 (E) or 35S (F). Proliferation of the synovial lining cells, erosive destruction of cartilage and bone and infiltration of inflammatory cells is noted in a joint of a 35S recipient (F) (H&E staining, ×40). (G) Gr-1-positive cells were abundant among the infiltrating cells in a joint of 35S recipient mouse (×200). High-magnification view (×1000) of the synovial lesion in 35S transferred mouse, showing that most of the infiltrating cells are granulocytes or monocytes (H) (H&E staining). (A, C and E) 12 months after transfer. (B, D and F–H) 10 months after transfer.

detected in every tested tissue with high frequency for the first 3 months after cell transfer; the detection rate became lower with time; clone-specific TCR signals were not detected in most tissues examined at 6–11 months after transfer, irrespective of the swelling of the joints and the presence of interstitial pneumonitis by histological examination. These findings collectively indicate that the T cell clones initiate arthritis but the progression and persistence of the disease may not require the expansion of the clones even if a small number of them might persist in the joints and the lung.

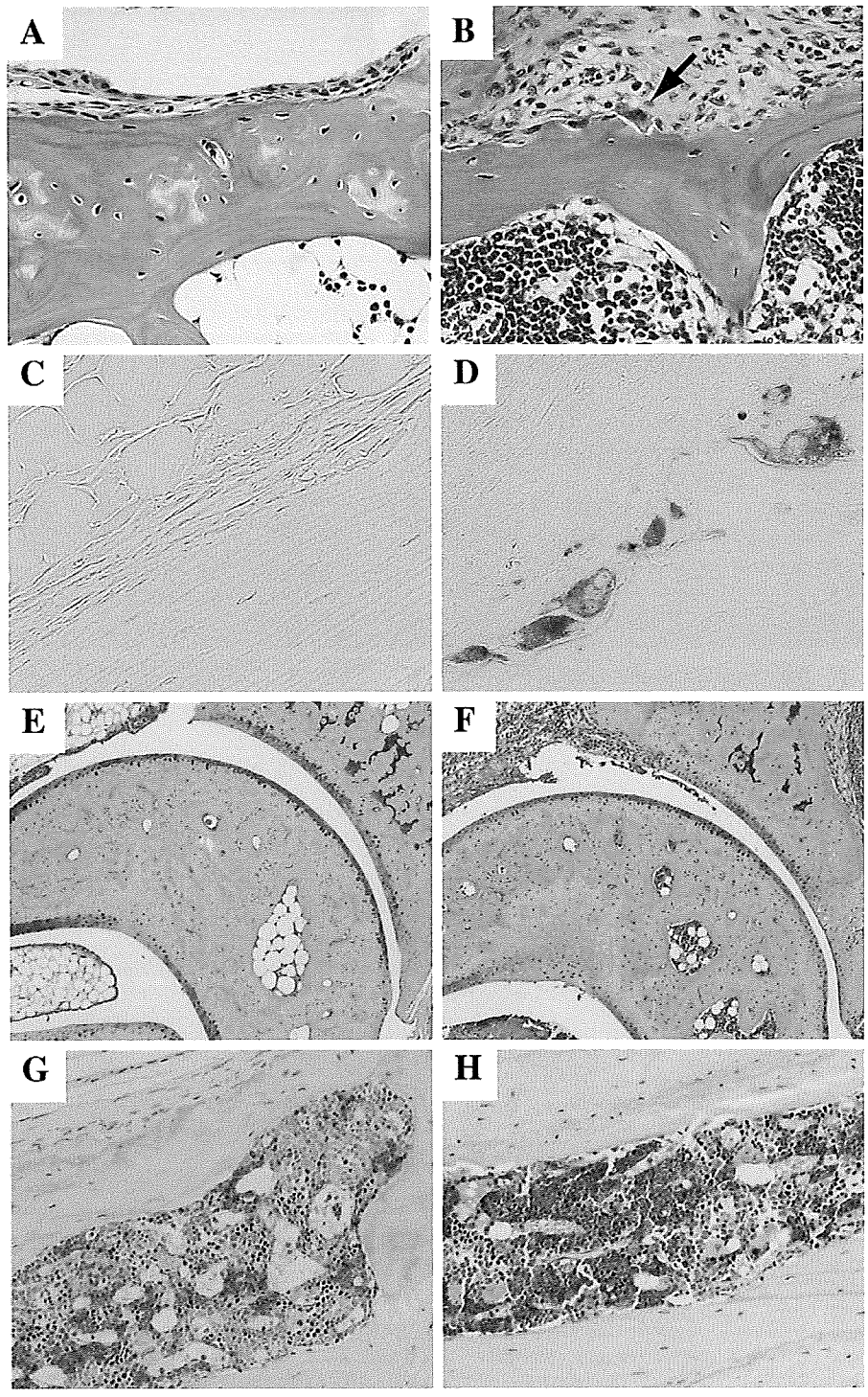

Fig. 6. Bone and cartilage destruction in athymic nude mice transferred with SKG T cell clones. High magnification of H&E-stained sections of a nude mouse recipient of dengue 2F7 (A) or 35S (B), showing bone erosion by pannus and BM activation (×400). Multinuclear cells (osteoclasts) (arrow) are also observed. Tartrate-resistant acid phosphatase-positive cells (osteoclasts) are detected in a 35S recipient (D) but not in a 2F7 recipient (C) (×400). By Safranin-O staining, proteoglycan stained red decreases in the articular cartilage matrix of a recipient of 35S (F) but not in a recipient of 2F7 (E) (×100). By immunohistochemistry, Gr-1-positive cells increase in the BM of a 35S recipient (H) but not in a 2F7 recipient (G) (×200). (A, C, E and G) 12 months after transfer; (B, D, F and H) 10 months after transfer.

Discussion

In this study, we have established two distinct $CD8^+$ T cell clones from arthritic lesions of SKG mice. Interestingly, both exhibited *in vitro* autoreactivity against not only synoviocytes but also a variety of MHC-matched cell lines and elicited both arthritis and interstitial pneumonitis when transferred to

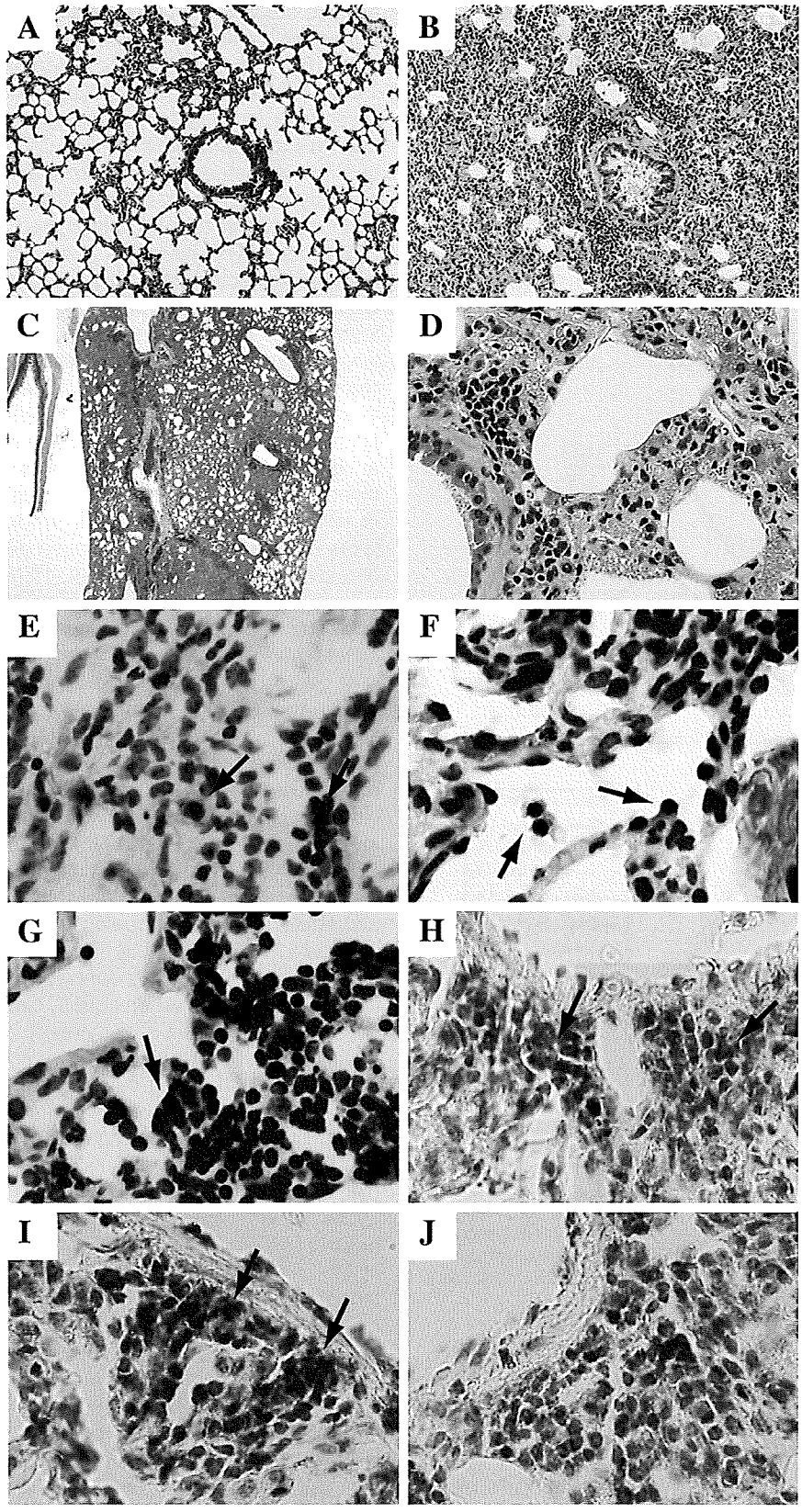

Fig. 7. Interstitial pneumonitis induced by the transfer of SKG T cell clones. (A–D) H&E-stained sections of the lungs of the recipients of control dengue 2F7 clone (A) or 73S clone (B–D) (A–B, ×100). Lower (C, ×10) and higher (D, ×400) magnification of the lung of 73S clone recipient show thickening of alveolar walls diffusely in the lung. (E–J) Serial sections of a lung of a 73S recipient mouse were stained for Ly-6G (Gr-1) (E), F4/80 (F), B220/CD45R (G), CD8a (H) or CD4 (I), with staining control (J) (×400). Typically positive cells in these stainings are arrowed. (A–J) 6 months after transfer.